



Synthesis, biological activity and multiscale molecular modeling studies of bis-coumarins as selective carbonic anhydrase IX and XII inhibitors with effective cytotoxicity against hepatocellular carcinoma

Belma Zengin Kurt^{a,*}, Aydan Dag^a, Berna Doğan^b, Serdar Durdagi^{b,*}, Andrea Angeli^c, Alessio Nocentini^c, Claudiu T. Supuran^c, Fatih Sonmez^d

^a *Bezmialem Vakif University, Faculty of Pharmacy, Department of Pharmaceutical Chemistry, 34093 Istanbul, Turkey*

^b *Computational Biology and Molecular Simulations Laboratory, Department of Biophysics, School of Medicine, Bahcesehir University, Istanbul, Turkey*

^c *Università degli Studi di Firenze, Dipartimento Neurofarba, Sezione di Scienze Farmaceutiche Nutraceutiche, Via U. Schiff 6, 50019 Sesto Fiorentino, Florence, Italy*

^d *Sakarya University of Applied Sciences, Pamukova Vocational Highschool, Pamukova, Turkey*

ARTICLE INFO

Keywords:

Coumarin
Carbonic anhydrase
Cytotoxicity
Molecular docking
Molecular Dynamics (MD) Simulations

ABSTRACT

A series of novel bis-coumarin derivatives containing triazole moiety as a linker between the alkyl chains was synthesized and their inhibitory activity against the human carbonic anhydrase (hCA) isoforms I, II, IX and XII were evaluated. In addition, cytotoxic effects of the synthesized compounds on renal adenocarcinoma (769P), hepatocellular carcinoma (HepG2) and breast adeno carcinoma (MDA-MB-231) cell lines were examined. While the hCA I and II isoforms were inhibited in the micromolar range, the tumor-associated isoform hCA IX and XII were inhibited in the high nanomolar range. 4-methyl-7-((1-(12-((2-oxo-2H-chromen-7-yl)oxy)dodecyl)-1H-1,2,3-triazol-4-yl)methoxy)-2H-chromen-2-one (**5p**) showed the strongest inhibitory activity against hCA IX with the K_i of 144.6 nM and 4-methyl-7-((1-(10-((2-oxo-2H-chromen-7-yl)oxy)decyl)-1H-1,2,3-triazol-4-yl)methoxy)-2H-chromen-2-one (**5n**) exhibited the highest hCA XII inhibition with the K_i of 71.5 nM. In order to better understand the inhibitory profiles of studied molecules, multiscale molecular modelling approaches were applied. Low energy docking poses of studied molecules at the binding sites of targets have been predicted. In addition, electrostatic potential surfaces (ESP) for binding sites were also generated to understand interactions between proteins and active ligands.

1. Introduction

Carbonic anhydrases (CAs, EC 4.2.1.1) are metalloenzymes, also known as carbonate dehydratases, which carry a zinc (II) ion from metal ions which are fundamental to catalysis [1]. CA, explored in the beef erythrocytes for the first time, reversibly catalyzes the reactions of hydration of CO₂ and dehydration of HCO₃⁻ [2,3]. The hydration of CO₂ occurs rather slowly without catalyst [4]. Carbonic anhydrases have been developed as six different enzyme families, α-, β-, γ-, δ-, ζ- and η-CAs. In mammals, sixteen α-CA isoenzymes or CA-related proteins (CARP) have been identified [5]. Their catalytic activities, intracellular localizations and tissue distributions are different. While CA I, CA II, CA III, CA VII and CA XIII are cytosolic, CA IV, CA IX, CA XII, CA XIV and CA XV are membrane-bound proteins. While CA VA and CA VB are mitochondrial proteins; CA VI shows intracellular localization as isozymes when saliva, milk and urine are secreted [6,7]. The three other

isoenzymes are termed CA related proteins without catalytic activity; CARP VIII, CARP X and CARP XI are found in the cytosol. Tissue distributions differ according to physiological/pathological conditions. While CA IX and XII isoenzymes are predominantly existing in hypoxic tumors, VA and XIV mainly are found in the liver. Carbonic anhydrases play a role in many pathological and physiological processes; transport of respiratory, CO₂, and bicarbonate between the metabolizing tissues and the lungs; pH and CO₂ homeostasis; secretion of electrolytes in various tissues and organs; biosynthesis reactions such as gluconeogenesis, lipogenesis; bone resorption; calcification; and tumor formation. Inhibition of CA isoenzyme; is important in the treatment of many diseases due to its role in diseases such as edema, glaucoma, obesity, cancer, epilepsy and osteoporosis [2,8].

Coumarins have a variety of pharmacological effects and they are mostly used in anticancer drug design and discovery [9]. The coumarins are a relatively new class of inhibitors of the metalloenzyme carbonic

* Corresponding authors.

E-mail addresses: bzengin@bezmialem.edu.tr (B.Z. Kurt), serdar.durdagi@med.bau.edu.tr (S. Durdagi).

<https://doi.org/10.1016/j.bioorg.2019.03.003>

Received 2 February 2019; Received in revised form 14 February 2019; Accepted 2 March 2019

Available online 07 March 2019

0045-2068/ © 2019 Published by Elsevier Inc.

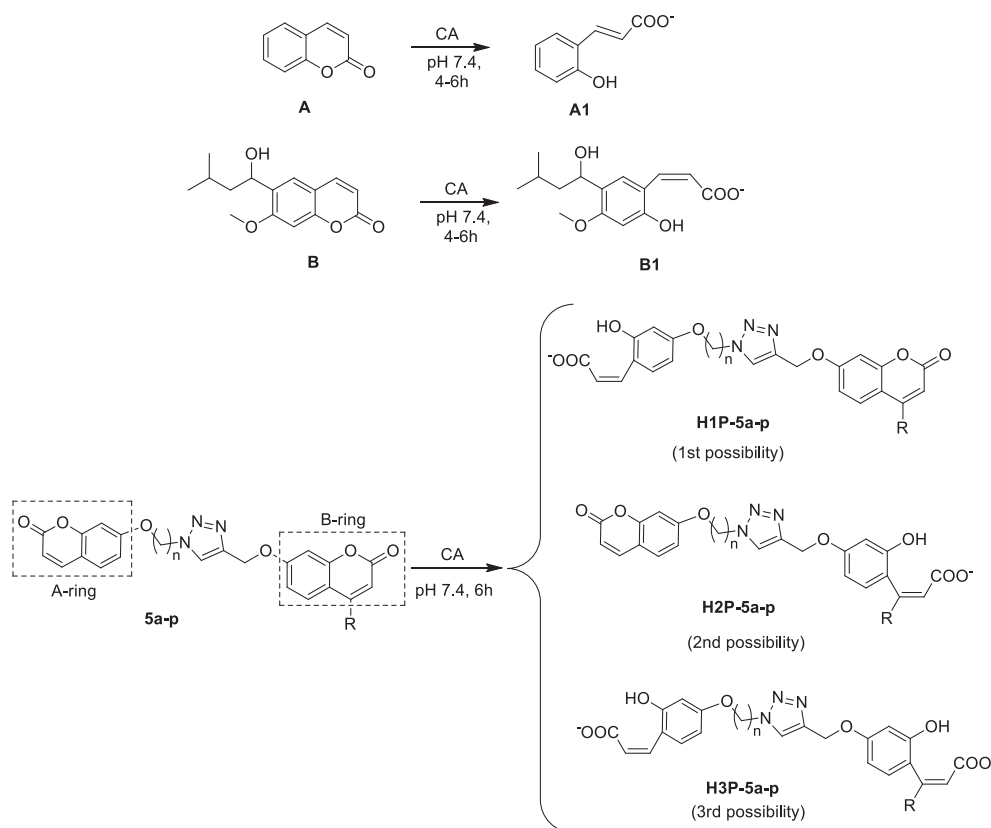


Fig. 1. Formation of 2-hydroxy-cinnamic acids A1, B1 and HP-5a-p by the CA-mediated hydrolysis of coumarin A, B and 5a-p.

anhydrase [10–12]. Coumarin and its bioisosteres (thiocoumarins, 2-thioxocoumarins) act as “prodrugs”, whereas their hydrolysis products (formed through CA-mediated esterase activity) are the actually CA inhibitors [13,14]. Many studies have shown that 7-hydroxycoumarin, 6-nitro-7-hydroxycoumarin, scopoletin and esculetin can be used in the treatment of cancer [15]. Coumarins demonstrate different mechanisms of antitumor activity at different stages of cancer formation. These mechanisms are; blockage of the cell cycle, apoptosis of the cell, blockage of the estrogen receptor, or inhibition of DNA-related enzymes such as topoisomerase [11].

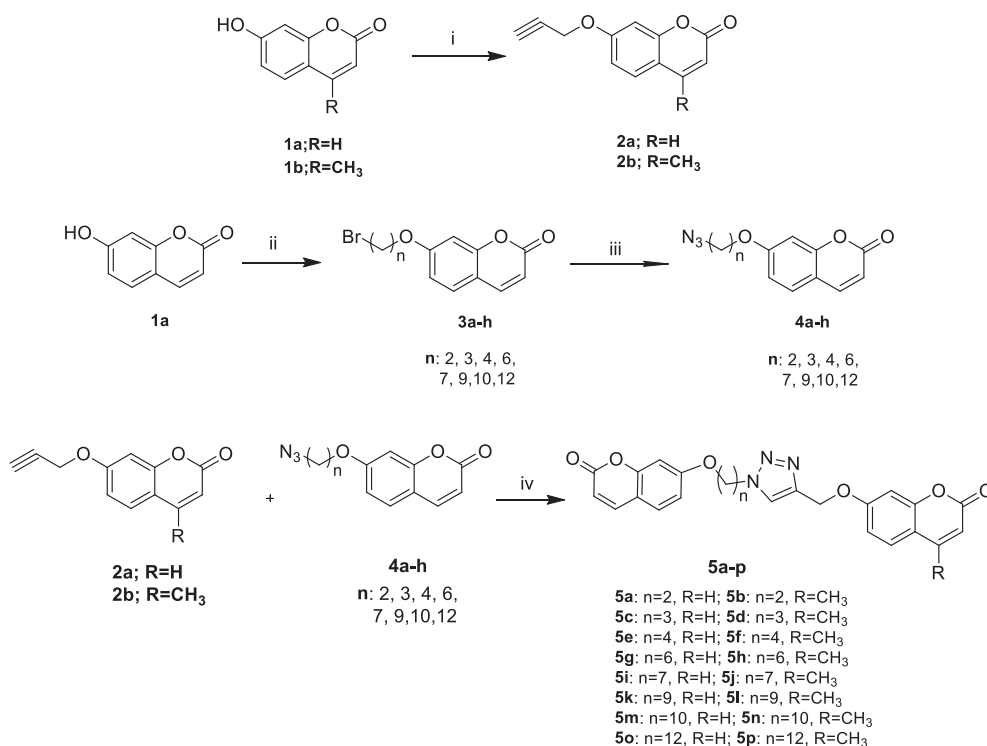
The key feature of most tumors is hypoxic. Hypoxia is inadequate oxygenation, resulting in pathologic consequences of tumor-damaged microcirculation and slowed oxygen diffusion [16,17]. Hypoxic tumor is more prone to spread, malignant development, chemotherapy and radiotherapy resistant. CA IX causes an increase in extracellular acidity catalyzed by the catalysis of bicarbonate and protons hydration of CO_2 , leads to the development of the acidic environment around the tumor and thus to the development of the tumor in the metastatic phenotype and the development of resistance to anticancer drugs [18,19]. Hypoxia inducible factor-1 (HIF-1) is induced effectively under hypoxic conditions, leading to the degradation of the expression and pH balance of CA IX and the development of classical chemotherapy and radiotherapy resistance [20]. In the studies performed, it was observed that continuous expression of CA-IX in the Madin-Darby canine kidney (MDCK) epithelial cell line reduced the extracellular pH (pHe). Low pH is associated with tumor-specific changes, chromosomal rearrangements, extracellular matrix breakdown, tumor migration and invasion, expression of cell growth factors and protease activation [21]. Hypoxia regulates the expression of most genes. CA IX expression is increased by hypoxia through HIF-1, while wild-type von Hippel-Lindau is reduced by tumor suppressor protein (pVHL) [22]. This increased expression of CA IX may be detected in tumors developing in glial and ependymal tissue, in mesothelioma, in papillary and follicular carcinomas, in bladder carcinomas, in uterine and cervical carcinomas, in nasopharynx

carcinomas, in head and neck carcinomas, in breast, oesophagus, lung, brain, vulva, and kidney tumors [23]. In some cancer cells, VHL gene mutation and HIF-1 activation were observed to cause the production of 150-fold more than the normal levels of CA-IX [24]. Thus, the inhibition of CA IX isoenzyme inhibits the tumor growth activity of CA IX in hypoxic tumors, controlling pH irregularity in tumors and enabling new applications in cancer diagnosis and treatment. Therefore, it is thought that inhibition of tumor associated CA IX and CA XII isoenzymes may play an important role in the generation of new anticancer drugs and may be effective against hypoxic tumors that cannot respond to conventional chemotherapy and radiotherapy [25].

Many different studies have been performed previously for the identification of selective inhibition of CA IX and XII enzymes. For example, Mollica et al. [26] have been synthesized novel probenecid-based amide derivatives including different natural amino acids and assayed to test their effect on the hCA IX and XII over the ubiquitous isoforms hCA I and II and most of the synthesized compounds were presented a complete loss of hCA II inhibition ($K_{is} > 10,000$ nM) and strong inhibitory activity against hCA IX and XII in the nanomolar range with respect to the parent compound. In another study D’Ascenzio et al. [27] have been synthesized a large number of novel secondary sulfonamides based on the open saccharin scaffold and evaluated as selective inhibitors of four different hCA I, II, IX and XII.

Also, some natural compounds and peptides have been previously recognized as activators of human and bacterial CAs [28,29].

As a continuation of our studies on coumarin CAIs, in this work aimed to achieve a more effective CA inhibition by performing double-ended synthesis of the coumarin molecule which is known to be effective on carbonic anhydrases. Therefore, we focus on two types of the coumarins possessing propargyl and azide moieties with different alkyl chains and they were combined via Copper (I) catalysed-Azide-Alkyne-Cycloaddition (CuAAC) reactions, known as Click reactions. Consequently, the novel sixteen bis-coumarin derivatives including different internal alkyl chains between two peripheral coumarin rings



Scheme 1. Synthesis of new triazole ring substituted bis-coumarin derivatives. Reaction conditions: (i) Propargylbromide, K₂CO₃, Acetone, 8h, reflux; (ii) Dibromide derivatives, K₂CO₃, CH₃CN, 2h, reflux; (iii) NaN₃, DMF, 8h, rt; (iv) CuBr, PMDETA, 12h, rt.

were synthesized by simple and efficient methods and their cytotoxic activity and effects on hCA isoforms were evaluated. Moreover, molecular modeling studies were also applied for better understanding the structural, dynamical and binding profiles of studied molecules at the active sites of targets. Specifically, molecular docking studies were carried out to clarify the inhibition mode for the studied compounds at the active sites of the target structures. Coumarin derivatives have been shown to hydrolyze with the increase of incubation times [30]. Hence, in addition to parent coumarin derivatives, the possible hydrolysis products shown in Fig. 1 were also considered. Predicted binding energies of these compounds and structural and dynamical profiles of molecules at the target sites were estimated using GOLD docking algorithm.

2. Result and discussion

2.1. Chemistry

The synthesis of the target compounds **5a-p** is depicted in Scheme 1. 7-hydroxycoumarin (**1a**) or 4-methyl-7-hydroxycoumarin (**1b**) was reacted with propargylbromide to obtain coumarin derivatives including alkyne moiety (**2a** and **2b**). On the other hand, 7-hydroxycoumarin (**1a**) was also reacted with alkyl bromides and then it was treated with sodium azide to get other components required for the synthesis of bis-coumarin. The coumarin derivatives containing alkyne moiety (**2a,b**) and azide moiety (**4a-h**) were combined via CuAAC reaction, known as Click reaction, to obtain bis-coumarin (**5a-p**) derivatives containing triazole rings.

All of these new compounds in this study were synthesized and characterized by ¹H NMR, ¹³C NMR, IR, MS and elemental analysis. According to the IR spectra of the synthesized bis-coumarin compounds, it was possible to observe the absorption peaks at about 2950 cm⁻¹ relating to CH stretch of aliphatic groups and absorption peaks at 1710–1740 cm⁻¹ from coumarin carbonyl moiety stretch. Additionally, because a triazole ring was generated along with the reaction of two coumarin molecules, the absorption peak of triazole ring

at 3130 cm⁻¹ represented the click reaction efficiency. From the ¹H NMR spectra; the signals for aromatic hydrogens were observed between 6.27 and 8.30 ppm, the signal of CH proton at triazole ring was detected at about 6.13–6.72 ppm and signals observed about 5.25 ppm belonged to –OCH₂ proton. In addition, the signals of aliphatic hydrogen atoms were determined between 1.00 and 4.50 ppm. From the ¹³C NMR spectra, the signals can be observed at about 161.5 and 162.5 ppm for carbonyl of lactone groups. The signals of the aliphatic and aromatic carbons were observed at 18–69 ppm and 101–161 ppm, respectively.

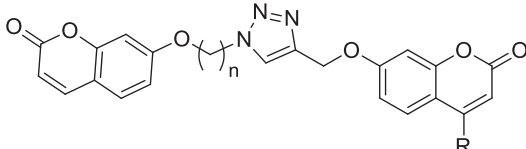
¹H NMR, ¹³C NMR, and MS spectra of the synthesized compounds are given in supplementary materials.

2.2. CA inhibition

The inhibition constants (K_i) of the synthesized compounds **5a-p** against hCA I, hCA II, hCA IX and hCA XII isoforms are given in Table 1. The tumour-associated isoform hCA IX and hCA XII were selectively inhibited by all the synthesized bis-coumarins with inhibition constants ranging from 71.5 nM to 2737.1 nM, while the hCA I and II isoforms were inhibited in the μM range. Among the synthesized bis-coumarins, **5p** had the highest inhibitory activity against hCA IX with a K_i of 144.6 nM and **5n** exhibited the strongest inhibition against hCA XII with a K_i of 71.5 nM.

Some notions about structure-activity relationship (SAR) emerged from these studies: (i) the presence of the methyl group on the coumarin ring decreased the inhibitory activity against hCA IX as the number of C in the linker is 2, 3, 4, or 6 (comparing **5a** (n = 2, R = H, K_i = 645.0 nM) with **5b** (n = 2, R = CH₃, K_i = 1253.0 nM); comparing **5c** (n = 3, R = H, K_i = 1312.3 nM) with **5d** (n = 3, R = CH₃, K_i = 1587.1 nM); comparing **5e** (n = 4, R = H, K_i = 1247.6 nM) with **5f** (n = 4, R = CH₃, K_i = 1833.3 nM); comparing **5g** (n = 6, R = H, K_i = 1054.5 nM) with **5h** (n = 6, R = CH₃, K_i = 1619.0 nM)), whereas it increased the hCA IX inhibition as the C number is 7, 9, 10 or 12 (comparing **5i** (n = 7, R = H, K_i = 2737.1 nM) with **5j** (n = 7, R = CH₃, K_i = 2115.9 nM); comparing **5k** (n = 9, R = H,

Table 1
In vitro inhibition K_i values (nM) of **5a-p** for the hCA I, II, IX and XII.



Compound	n	R	K_i (nM) ^a			
			hCA I	hCA II	hCA IX	hCA XII
5a	2	H	> 10000	> 10000	645.0	587.5
5b	2	CH ₃	> 10000	> 10000	1253.0	635.7
5c	3	H	> 10000	> 10000	1312.3	509.7
5d	3	CH ₃	> 10000	> 10000	1587.1	409.6
5e	4	H	> 10000	> 10000	1247.6	554.9
5f	4	CH ₃	> 10000	> 10000	1833.3	770.5
5g	6	H	> 10000	> 10000	1054.5	852.3
5h	6	CH ₃	> 10000	> 10000	1619.0	891.5
5i	7	H	> 10000	> 10000	2737.1	704.7
5j	7	CH ₃	> 10000	> 10000	2115.9	546.0
5k	9	H	> 10000	> 10000	1969.7	608.1
5l	9	CH ₃	> 10000	> 10000	1154.1	649.7
5m	10	H	> 10000	> 10000	2675.4	648.3
5n	10	CH ₃	> 10000	> 10000	160.9	71.5
5o	12	H	> 10000	> 10000	211.1	415.3
5p	12	CH ₃	> 10000	> 10000	144.6	785.2
AAZ	–	–	250	12.1	25.8	5.7

^a Mean from 3 different assays, by a stopped flow technique (errors were in the range of \pm 5–10% of the reported values).

$K_i = 1969.7$ nM) with **5l** ($n = 9$, $R = \text{CH}_3$, $K_i = 1154.1$ nM); comparing **5m** ($n = 10$, $R = \text{H}$, $K_i = 2675.4$ nM) with **5n** ($n = 10$, $R = \text{CH}_3$, $K_i = 160.9$ nM); comparing **5o** ($n = 12$, $R = \text{H}$, $K_i = 211.1$ nM) with **5p** ($n = 12$, $R = \text{CH}_3$, $K_i = 144.6$ nM). (ii) while R is H or CH_3 , and the linker is the dodecanyl ($n = 12$), the best hCA IX inhibitions were observed (**5o** ($n = 12$, $R = \text{H}$, $K_i = 211.1$ nM) and **5p** ($n = 12$, $R = \text{CH}_3$, $K_i = 144.6$ nM)). On the otherhand **5n** ($n = 10$, $R = \text{CH}_3$) had the highest hCA XII inhibitory activity ($K_i = 71.5$ nM). (iii) The increasing number of C in the linker moiety from two to three and from six to seven led to a decline the inhibitory activity against hCA IX (comparing **5a** ($n = 2$, $R = \text{H}$, $K_i = 645.0$ nM) with **5c** ($n = 3$, $R = \text{H}$, $K_i = 1312.3$ nM); comparing **5b** ($n = 2$, $R = \text{CH}_3$, $K_i = 1253.0$ nM) with **5d** ($n = 3$, $R = \text{CH}_3$, $K_i = 1587.1$ nM); comparing **5g** ($n = 6$, $R = \text{H}$, $K_i = 1054.5$ nM) with **5i** ($n = 7$, $R = \text{H}$, $K_i = 2737.1$ nM); comparing **5h** ($n = 6$, $R = \text{CH}_3$, $K_i = 1619.0$ nM) with **5j** ($n = 7$, $R = \text{CH}_3$, $K_i = 2115.9$ nM)), whereas it increased the inhibitory activity against hCA XII (comparing **5a** ($n = 2$, $R = \text{H}$, $K_i = 587.5$ nM) with **5c** ($n = 3$, $R = \text{H}$, $K_i = 509.7$ nM); comparing **5b** ($n = 2$, $R = \text{CH}_3$, $K_i = 635.7$ nM) with **5d** ($n = 3$, $R = \text{CH}_3$, $K_i = 409.6$ nM); comparing **5g** ($n = 6$, $R = \text{H}$, $K_i = 852.3$ nM) with **5i** ($n = 7$, $R = \text{H}$, $K_i = 704.7$ nM); comparing **5h** ($n = 6$, $R = \text{CH}_3$, $K_i = 891.5$ nM) with **5j** ($n = 7$, $R = \text{CH}_3$, $K_i = 546.0$ nM)). Additionally, while R is CH_3 , the increasing number of C in the linker moiety from nine to ten dramatically increased the inhibitory activity against both hCA IX and hCA XII (comparing **5l** ($n = 9$, $R = \text{CH}_3$, $K_i = 1154.1$ nM and 649.7 nm against hCA IX and hCA XII, respectively) with **5n** ($n = 10$, $R = \text{CH}_3$, $K_i = 160.9$ nM and 71.5 nm against hCA IX and hCA XII, respectively)). Although there is no a linear relation between increasing C number of the alkyl group and inhibitor activity, the best inhibitors against the tumor-associated hCA IX and hCA XII have the longer alkyl chain (C number of 10 and 12). It can be hypothesized that the long alkyl chain as a linker provides different molecular conformations and intra-molecular movement ability as shown in Figs. 2 and 4, therefore, both terminal coumarin moieties of the synthesized compounds can effectively interact with the active sites of the enzyme.

It is known that coumarins are mechanism-based inhibitors, which

undergo hydrolysis under the influence of the zinc-hydroxide, nucleophilically active species of the enzyme, with generation of substituted-2-hydroxycinnamic acids (Fig. 1) [30–34]. It was reported that coumarin/thiocoumarin inhibitors and enzyme solutions were pre-incubated together before assay to form the E-I complex or for the ultimate active site mediated hydrolysis of the inhibitor [35]. Based on these researches, it can be considered that the synthesized bis-coumarin should hydrolyse to cinnamic acid derivative during pre-incubation on enzyme and inhibitor via three different possibilities as opening the only coumarin A-ring, opening the only coumarin B-ring and opening both coumarin rings (Fig. 1). If the pre-incubation time and the concentration of the zinc-hydroxide are sufficient for hydrolyzing of the bis-coumarins, opening both coumarin rings can be considered as the highest possibility.

2.3. Cell cytotoxicity

On basis of the screening results above, all of the synthesized compounds were examined to specify their potential cytotoxicity effect towards many cancerous cell lines. Accordingly, the renal cell adenocarcinoma (769P), liver hepatocellular carcinoma (HepG2) and breast adenocarcinoma (MDA-MB-231) cell lines were treated with different doses of the synthesized compounds (**5a-p**) for 24 h in complete medium. The cell viability was evaluated by the 3-(4,5-dimethylthiazol-2-yl)-2,5-diphenyltetrazolium (MTT) assay. The cytotoxicity effect (IC_{50}) of the synthesized compounds (**5a-p**) against 769P, HepG2 and MDA-MB-231 cell lines are given in Table 2. In general, the IC_{50} values of the synthesized compounds were effective in the range between 0.383 μM and 13.552 μM on cancer cell lines. Additionally, compound **5g** showed the strongest cytotoxic effect against 769P cell line with an IC_{50} value of 2.026 μM and **5k** exhibited the strongest cytotoxic effect against MDA-MB-231 with an IC_{50} value of 1.239 μM . Furthermore, compound **5a** showed the strongest cytotoxic effect against HepG2 with an IC_{50} value of 0.383 μM , which is almost 2-fold more than that of Doxorubicin used as a standard.

2.4. Molecular modeling

The docking scores of the studied compounds at the binding pockets of CA-IX and XII targets along with their hydrolyzed products are shown in Table 3. Short MD simulations (10 ns) were performed for the targets before the docking and the trajectories obtained by simulations were clustered. The representative structure from the cluster with the largest size was taken as initial complex structure for docking studies. In all cases except **5k** for hCA IX, at least one of the hydrolyzed derivatives, i.e. cinnamic acid derivatives are predicted to have higher fitness score which means that more promising docking pose. In this sense, the docking results for all compounds except **5k** for hCA IX are in good agreement that hydrolyzed coumarin derivatives have lower inhibition concentrations than that of coumarins as presented by Maresca et al. [30,31]. For isoform hCA IX the highest fitness score is predicted for H3P-5p which is shown to be the most promising inhibitor with lowest K_i experimentally (Table 1). In fact, the three compounds with the lowest inhibition constant namely **5n**, **5o**, **5p** and/or their hydrolyzed products were also the highest potential compounds based on the docking results. The electrostatic potential surfaces (EPS) of these highest scoring docking poses for H3P-5p along with 2D ligand interaction diagram can be found in Fig. 2. Based on top-docking pose, Trp141 and Thr333 form hydrogen bonds with the ligand. While the red colored regions show fields with negative partial atomic charges, blue colored regions show fields with positive partial atomic charges. EPS of compound **5i**, one of the molecules that shows low inhibition against isoform IX is also shown in Fig. 3. It can be argued that while compound **5p** derivative H3P-5p fits into the target site without clashes and/or repulsion between protein and ligand, there is some repulsion for H3P-5i ligand-protein complex (i.e., close red-colored regions can be

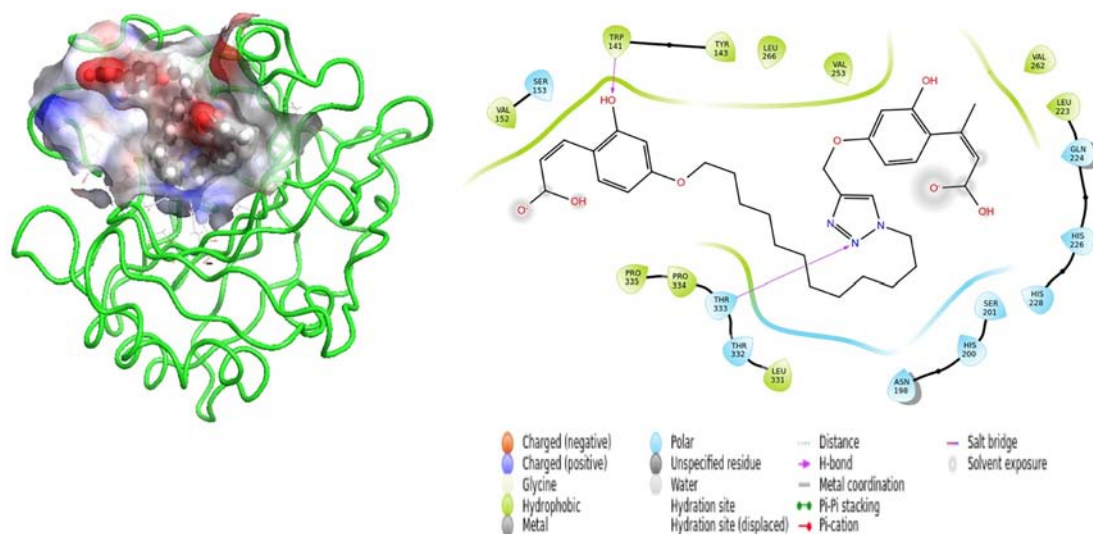


Fig. 2. (left) Electrostatic potential map for H3P-5p and hCA IX complex highest scoring docking pose. (right) 2D ligand interaction diagram for docked ligand. The ligand is shown as CP2K representation, binding site residues are shown as lines.

Table 2

Summary of IC₅₀ values of **5a-p** towards 769P, HepG2 and MDA-MB-231 cell lines.

Compound	IC ₅₀ (μM)		
	769P	HepG2	MDA-MB-231
5a	3.330 ± 0.008	0.383 ± 0.007	9.411 ± 0.006
5b	7.692 ± 0.013	1.023 ± 0.011	6.477 ± 0.009
5c	7.013 ± 0.010	1.073 ± 0.008	6.264 ± 0.006
5d	10.610 ± 0.009	1.252 ± 0.006	10.648 ± 0.006
5e	11.341 ± 0.012	1.726 ± 0.009	10.973 ± 0.006
5f	6.772 ± 0.011	3.025 ± 0.009	4.892 ± 0.005
5g	2.026 ± 0.007	1.219 ± 0.009	10.219 ± 0.004
5h	6.743 ± 0.007	1.563 ± 0.015	8.777 ± 0.003
5i	7.181 ± 0.010	3.274 ± 0.007	10.219 ± 0.004
5j	6.814 ± 0.011	6.200 ± 0.010	8.777 ± 0.003
5k	4.763 ± 0.020	3.034 ± 0.006	1.239 ± 0.003
5l	6.073 ± 0.022	3.806 ± 0.005	1.664 ± 0.002
5m	2.489 ± 0.012	2.585 ± 0.014	8.505 ± 0.006
5n	3.194 ± 0.011	4.739 ± 0.015	9.063 ± 0.005
5o	9.096 ± 0.011	1.387 ± 0.010	11.249 ± 0.007
5p	7.580 ± 0.011	1.260 ± 0.013	13.552 ± 0.007
Doxorubicin	0.450 ± 0.040	0.820 ± 0.090	0.890 ± 0.660

interpreted as repulsive forces between ligand and receptor sites). For isoform hCA XII, *in vitro* results showed that all compounds except **5n** show similar inhibition (Table 1). In our docking simulations we also found that mainly all compounds have similar docking scores. However, surprisingly compound **5l**'s H2P-5l form showed slightly higher score compared to others. The 2D ligand interaction diagram of predicted docking pose for the **5n** product H1P-5n is shown in Fig. 4 along with the EPS of the complex. Based on interaction diagram, H1P-5n forms following H-bonds with the target protein: Tyr6, Asn64, Lys69, Thr88, and Gln89. Lys69 also forms salt bridge interactions with the ligand.

It is already well-established that designing inhibitors with selectivity against specific isoforms of hCA is very challenging due to the sequence and structure similarity between isoforms [2,4]. In Fig. 5, the sequence alignment of hCA isoforms I, II, IX and XII is shown. Here only the catalytic domains of enzymes are considered for all isoforms, hence transmembrane domain of hCA IX and hCA XII are ignored. Residue numbers are taken from PDB structures with codes 5E2M for hCA-I, 3F8E for hCA-II, 5DVX for hCA-IX and 5MSA for hCA-XII. Secondary

structures assignments (SSA) along with disulfide bonds (SSBOND) are also displayed in Fig. 5 for each protein structures. The residues are colored based on their hydrophobicity. As it can be seen from this figure, secondary structures of all considered isoforms are almost same and this situation is clearer especially at the catalytic site (i.e., residue numbers 92, 94, 96, 106, 120–122, and 200–205 in Fig. 5.) where sulfonamide inhibitors bind, no selectivity could be achieved as the residues of the catalytic sites are almost same in all considered isoforms. Hence, Maresca et al. suggested a new binding site that is on the entrance to the enzyme binding site which is also the region with most variation in amino acid sequences and it would be possible to design inhibitors with selectivity against specific isoforms of hCA [30–32,36]. These coumarin binding sites are tentatively shown in Fig. 6. The 3D structures of isoforms (from above mentioned PDB codes) are aligned and specifically the coumarin binding site is assessed. It can be seen that there are important variations in amino acid side chains on these coumarin sites of considered isoforms, specifically residues with sequence numbers 6, 67, 69 and 133 Fig. 5.

3. Conclusion

In conclusion, 16 novel bis-coumarin derivatives containing triazole ring and alkyl chain (**5a-p**) are synthesized and their effects on the hCA I, II, IX and XII isoforms are evaluated. All the synthesized compounds exhibited selective inhibitory activity in the high nM range against the tumor-associated isoform hCA IX and hCA XII. Among them, **5p** showed the strongest inhibitory activity against hCA IX with the K_i of 144.6 nM and **5n** exhibited the highest hCA XII inhibition with the K_i of 71.5 nM. Furthermore, cytotoxic effects of the synthesized compounds on renal adenocarcinoma (769P), hepatocellular carcinoma (HepG2) and breast adeno carcinoma (MDA-MB-231) cell lines are examined. The results revealed that they exhibited very good anticancer properties especially in the hepatocellular carcinoma (HepG2) cell line between cytotoxicity experiments performed on 3 different cell lines. **5a** showed the strongest cytotoxic effect against HepG2 with an IC₅₀ value of 0.383 μM, which is almost 2-fold more than that of Doxorubicin used as a standard.

Multiscale molecular modeling approaches are used to investigate binding poses and predicted binding energies of studied compounds (both hydrolyzed and non-hydrolyzed forms) at the active sites of the CA IX, and XII isoforms. The docking studies were in general agreement that hydrolyzed products of synthesized compounds would interact

Table 3
Docking scores for compounds of **5a-p** and their hydrolysis products HP-5a-p for the hCA IX and XII.

Compound	Docking Score (CHEMPLP)	
	hCA IX	hCA XII
5a	74.34	82.81
H1P-5a	77.45	85.07
H2P-5a	80.03	85.82
H3P-5a	81.87	85.82
5b	76.26	75.88
H1P-5b	78.72	84.92
H2P-5b	78.74	78.84
H3P-5b	82.86	84.17
5c	75.20	85.38
H1P-5c	79.29	84.96
H2P-5c	77.59	86.06
H3P-5c	81.62	90.52
5d	78.01	75.48
H1P-5d	76.86	85.23
H2P-5d	83.62	79.12
H3P-5d	76.56	96.12
5e	81.52	79.64
H1P-5e	78.32	87.06
H2P-5e	78.48	85.54
H3P-5e	86.73	90.28
5f	79.16	78.25
H1P-5f	81.85	87.06
H2P-5f	83.11	82.73
H3P-5f	83.24	85.06
5g	83.78	80.39
H1P-5g	87.65	90.56
H2P-5g	83.47	89.41
H3P-5g	85.18	92.77
5h	82.63	81.83
H1P-5h	86.97	92.08
H2P-5h	83.65	85.19
H3P-5h	80.57	97.76
5i	84.56	86.32
H1P-5i	84.25	91.36
H2P-5i	85.47	92.23
H3P-5i	84.03	100.24
5j	79.15	88.39
H1P-5j	84.29	95.04
H2P-5j	83.15	84.03
H3P-5j	88.19	93.38
5k	86.44	82.13
H1P-5k	82.09	91.02
H2P-5k	84.57	93.58
H3P-5k	85.25	94.15
5l	86.18	84.69
H1P-5l	86.84	98.68
H2P-5l	84.57	104.87
H3P-5l	85.25	91.25
5m	82.88	84.79
H1P-5m	83.64	88.25
H2P-5m	87.18	92.23
H3P-5m	84.49	88.01
5n	87.34	90.53
H1P-5n	85.25	96.01
H2P-5n	82.14	87.74
H3P-5n	90.40	92.62
5o	90.04	82.31
H1P-5o	90.49	90.90
H2P-5o	90.22	94.57
H3P-5o	88.09	95.12
5p	87.99	86.00
H1P-5p	90.56	91.26
H2P-5p	89.04	92.35
H3P-5p	92.13	91.75

with the target site better compared to coumarin derivatives as for each compound, the highest docking scores are for compounds with at least one coumarin ring open. Docking results showed the highest docking scores for **5n**, **5o** and **5p** compared to other compounds at the hCA IX.

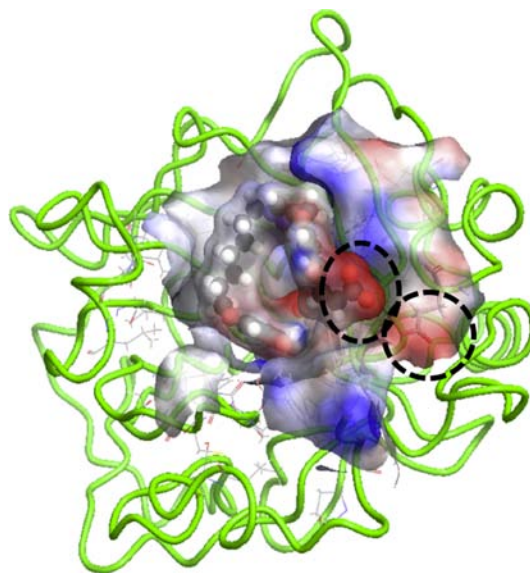


Fig. 3. Electrostatic potential map for H3P-5i and hCA IX complex. The ligand is shown as CP2K representation, binding site residues are shown as lines. Protein is represented as ribbon. Compound 5i shows lowest activity at the hCA IX, and its low activity can be due to repulsive forces between ligand and target (labeled regions at the Figure).

4. Experimental

4.1. Material and method

Melting points were taken on a STUART SMP40. IR spectra were measured on Alfa Bruker spectrometer. ^1H and ^{13}C NMR spectra were measured on a Varian Infinity Plus spectrometer at 300 and at 75 Hz, respectively. ^1H and ^{13}C chemical shifts are referenced to the internal deuterated solvent. Mass spectra were obtained using MICROMASS Quattro LC-MS-MS spectrometer. The elemental analyses were carried out with a Leco CHNS-932 instrument. Spectrophotometric analyses were performed by a BioTek Power Wave XS (BioTek, USA). The cell line was purchased from American Type Culture Collection (ATCC). Dulbecco's Modified Eagle's Medium-F12, RPMI Medium, fetal calf serum, and PBS were purchased from GIBCO BRL, InVitrogen (Carlsbad, CA). The chemicals and solvents were purchased from Fluka Chemie, Merck, Alfa Aesar and Sigma-Aldrich.

4.2. General procedures and spectral data

4.2.1. 4-methyl-7-(prop-2-yn-1-yloxy)-2H-chromen-2-one (2a-b)

To a solution of 7-hydroxycoumarin or 4-methyl-7-hydroxycoumarin (1.00 g, 6.17 mmol) in acetone (40 mL), propargyl bromide (0.88 g, 7.40 mmol) and anhydrous K_2CO_3 (1.00 g) were added. The mixture was refluxed for 8 h, and then it was hot filtered and concentrated under reduced pressure. The crude was crystallized with petroleum ether, affording (95–97%) of **2a-b** [37].

4.2.2. General procedure for the synthesis of 3a-h

K_2CO_3 (12 mmol) and dibromide derivatives (6 mmol) were added to a solution of **1a** (2 mmol) in CH_3CN (20 mL). The reaction mixture was refluxed for 2 h. Upon completion, K_2CO_3 was removed by filtration and the solvent was concentrated under vacuum, the residue was dissolved in CH_2Cl_2 , washed with water, brine, dried over anhydrous Na_2SO_4 and concentrated under vacuum to give compounds **3a-h** and purification column chromatograph (Eluent; Hexane-EtOAc; 4:1) [38].

7-(2-bromoethoxy)-2H-chromen-2-one (**3a**). White powder, 42% yield; IR: 3081, 1727, 1711, 1605, 1556, 1508, 1393, 1353, 1268, 1226, 1202, 1122, 1096, 1010, 990, 891, 831, 806, 760, 615, 572, 546,

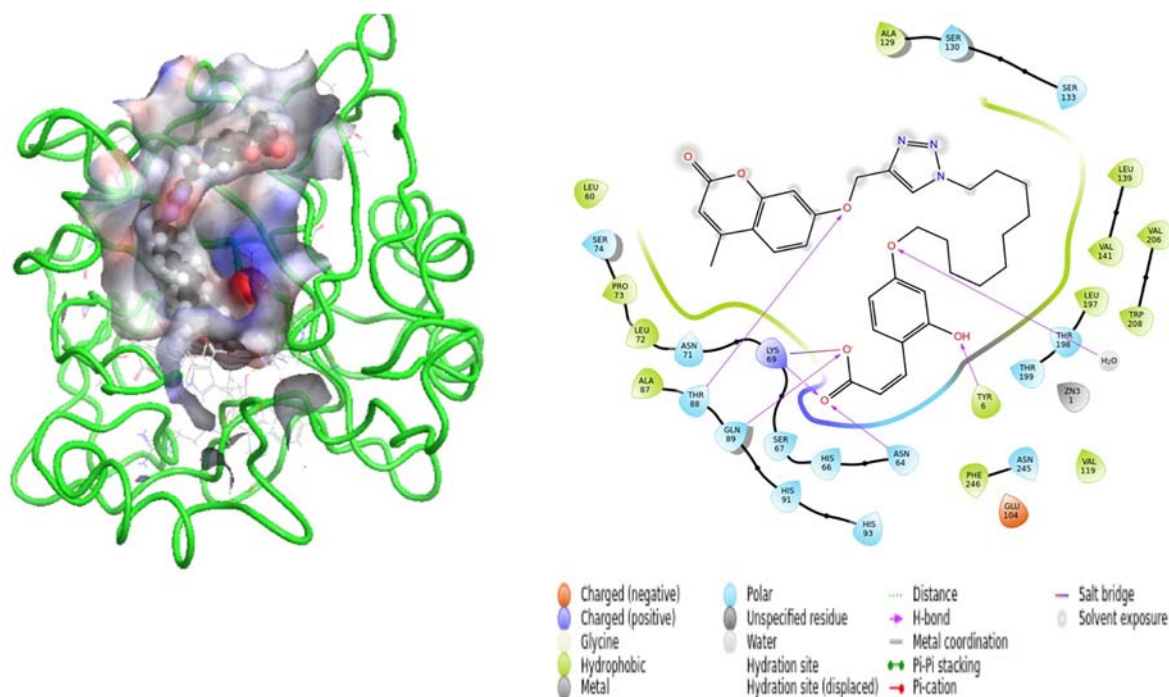


Fig. 4. Electrostatic potential map for H1P-5n and hCA XII complex. On the right, 2D ligand interaction diagram along for docked ligand. The ligand is shown as CP2K representation, binding site residues shown as lines. Protein is represented as ribbon.

Name	Sequence	HOM%
hCA I (5E2M)_A	1 10 20 30 40 50 60 70 80 5 -WGYDITGPVWSLWYPAACGHSPLVITLTSVPLSS--YIPATAITLGGSLVITVDDVSYIT 80	100%
hCAII (3F8E)_A	4 -WGYCITGPVWVWVPPAAGHSPLVITLTSVPLSS--YIATSITLGGSLVITVDDVSYITAVI 80	71%
hCA IX (5DVX)_A	140 -WVYGG---PPWFVSPACAFVSPVWVPLAAFCPALPLVIGFVPPVPLVGGSLVITVDDVSYITMAG- 215	46%
hCA XII (5MSA)_A	3 -WTYRGPVGSWSLYPSCGCTVSPVWVSLVLYASVPLVFGYLSANVGFVITVGGSLVITVDDVSYITM 81	51%
hCA I (5E2M)_A	81 90 100 110 120 130 140 150 160 GGPFSYVDFVFWGSLVNGSHTVYVYSAITVAWVSAVSSAAARSAGAVVGVVAVGVAAPV 158	100%
hCAII (3F8E)_A	81 GGPVIGTYVDFVFWGSLVNGSHTVYVYVYAAVAVVWV-TVYVGVAVVAVVAVVAVVAVVAVVAVV 158	71%
hCA IX (5DVX)_A	216 ---VGVYVAVV 290	46%
hCA XII (5MSA)_A	82 ---VSAVAVV 156	51%
hCA I (5E2M)_A	159 170 180 190 200 210 220 230 240 VVIATVAVV 235	100%
hCAII (3F8E)_A	159 VVVVAVV 235	71%
hCA IX (5DVX)_A	291 VVLSVAVV 365	46%
hCA XII (5MSA)_A	157 VVESHVAVV 236	51%
hCA I (5E2M)_A	236 250 260 270 280 290 300 310 320 AVV 260	100%
hCAII (3F8E)_A	236 VVVAVV 260	71%
hCA IX (5DVX)_A	366 VVAVV 391	46%
hCA XII (5MSA)_A	237 VVAVV 262	51%

Fig. 5. Alignment of amino acid sequences for hCA I, II, IX and XII colored according to hydrophobicity of amino acids.

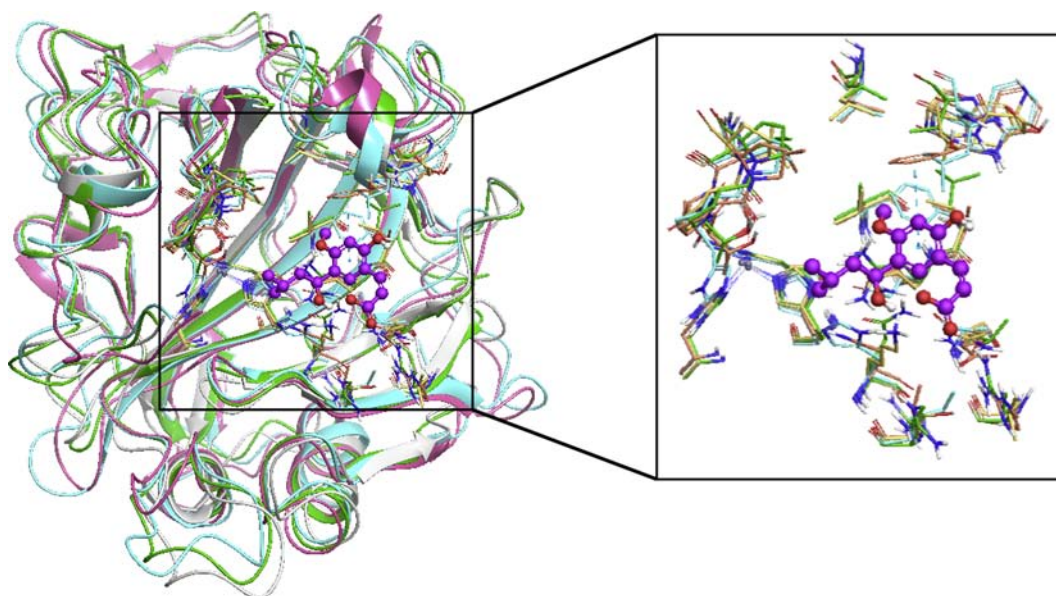


Fig 6. (left) Alignment of isoforms I, II, IX and XII of hCA. (right) The detailed binding site is shown. Binding site residues are represented by different colors: cyan for hCA I, orange for hCAII, green for hCA IX and yellow for hCA XII. The blue colored dashed line shows the pi-pi stacking interaction between Phe131 and phenyl ring of coumarin and yellow dashed lines show the hydrogen bonds. (For interpretation of the references to colour in this figure legend, the reader is referred to the web version of this article.)

483, 461 cm^{-1} ; ^1H NMR (DMSO- d_6 , 300 MHz) δ/ppm : 3.84 (2H, s, br), 4.40 (2H, s, br), 6.31 (1H, dd, $J = 2.6$ Hz, 9.3 Hz), 6.97–7.04 (2H, m), 7.64 (1H, d, $J = 8.4$ Hz), 8.0 (1H, dd, $J = 2.0$ Hz, 9.6 Hz); ^{13}C NMR (DMSO- d_6 , 75 MHz) δ/ppm : 31.7, 69.0, 102.1, 112.9, 113.4, 130.3, 144.9, 156.0, 160.9, 161.6, 162.6.

7-(3-bromopropoxy)-2H-chromen-2-one (3b). White powder, 71% yield; IR: 3068, 2951, 2863, 1701, 1603, 1552, 1400, 1290, 1238, 1147, 1128, 1038, 833, 749, 717, 614, 572, 549, 460 cm^{-1} ; ^1H NMR (DMSO- d_6 , 300 MHz) δ/ppm : 2.23–2.28 (2H, m), 3.66 (2H, t, $J = 6.4$ Hz), 4.17 (2H, t, $J = 5.8$ Hz), 6.28 (1H, d, $J = 9.4$ Hz), 6.95 (1H, d, $J = 8.4$ Hz), 7.0 (1H, s), 7.61 (1H, d, $J = 8.4$ Hz), 7.97 (1H, d, $J = 9.3$ Hz); ^{13}C NMR (DMSO- d_6 , 75 MHz) δ/ppm : 57.7, 66.0, 66.7, 101.7, 101.9, 130.2, 145.0, 156.0, 160.9, 161.0, 162.5.

7-(4-bromobutoxy)-2H-chromen-2-one (3c). White powder, 54% yield; IR: 3080, 2952, 2925, 2879, 1703, 1610, 1553, 1509, 1399, 1289, 1235, 1128, 1100, 1011, 826, 718, 614, 559, 457 cm^{-1} ; ^1H NMR (DMSO- d_6 , 300 MHz) δ/ppm : 1.91 (4H, s, br), 3.51 (2H, s, br), 4.16 (2H, s, br), 6.28 (2H, d, $J = 9.3$ Hz), 6.93–7.0 (2H, m), 7.63 (1H, d, $J = 8.7$ Hz), 8.0 (1H, d, $J = 9.3$ Hz); ^{13}C NMR (DMSO- d_6 , 75 MHz) δ/ppm : 25.7, 61.2, 68.5, 101.8, 112.9, 113.1, 113.4, 130.1, 145.0, 156.0, 161.0, 162.4.

7-((6-bromohexyl)oxy)-2H-chromen-2-one (3d). White powder, 60% yield; IR: 3080, 3049, 2942, 2861, 1719, 1610, 1555, 1507, 1467, 1393, 1287, 1234, 1127, 1098, 1033, 1001, 890, 825, 716, 640, 631, 615, 567, 515, 456 cm^{-1} ; ^1H NMR (DMSO- d_6 , 300 MHz) δ/ppm : 1.39–1.44 (4H, m), 1.69–1.82 (4H, m), 3.51 (2H, t, $J = 6.7$ Hz), 4.04 (2H, t, $J = 6.4$ Hz), 6.25 (1H, d, $J = 9.6$ Hz), 6.89–6.95 (2H, m), 7.59 (1H, d, $J = 8.4$ Hz), 7.96 (1H, d, $J = 9.3$ Hz); ^{13}C NMR (DMSO- d_6 , 75 MHz) δ/ppm : 32.8, 33.1, 35.8, 61.2, 68.8, 101.7, 112.9, 113.0, 130.1, 145.0, 156.0, 161.0, 162.5.

7-((7-bromoheptyl)oxy)-2H-chromen-2-one (3e). White powder, 65% yield; IR: 3065, 2937, 1745, 1611, 1554, 1399, 1289, 1131, 1098, 1028, 865, 845, 724 cm^{-1} ; ^1H NMR (DMSO- d_6 , 300 MHz) δ/ppm : 1.26–1.37 (7H, m), 1.66–1.77 (3H, m), 3.34 (1H, t, $J = 6.4$ Hz), 3.48 (1H, t, $J = 6.4$ Hz), 4.01 (2H, t, $J = 6.4$ Hz), 6.23 (1H, d, $J = 9.6$ Hz), 6.87–6.91 (2H, m), 7.57 (1H, d, $J = 8.4$ Hz), 7.94 (1H, d, $J = 9.3$ Hz); ^{13}C NMR (DMSO- d_6 , 75 MHz) δ/ppm : 26.1, 28.4, 29.3, 33.1, 35.8, 61.3, 68.8, 101.7, 112.8, 113.0, 113.3, 130.1, 145.0, 156.0, 161.0, 162.5.

7-(9-bromononyl)oxy)-2H-chromen-2-one (3f). White powder,

74% yield; IR: 3080, 2918, 1729, 1615, 1552, 1470, 1293, 1237, 1131, 1013, 845, 722 cm^{-1} ; ^1H NMR (DMSO- d_6 , 300 MHz) δ/ppm : 1.21–1.72 (11H, m), 2.47–2.48 (3H, m), 3.32 (1H, t, $J = 6.1$ Hz), 3.46 (1H, t, $J = 6.7$ Hz), 4.00 (2H, t, $J = 6.1$ Hz), 6.23 (1H, d, $J = 9.6$ Hz), 6.86–6.91 (2H, m), 7.57 (1H, d, $J = 8.4$ Hz), 7.95 (1H, d, $J = 9.3$ Hz); ^{13}C NMR (DMSO- d_6 , 75 MHz) δ/ppm : 26.1, 28.1, 29.1, 29.4, 29.7, 33.2, 35.8, 61.3, 68.8, 101.6, 112.8, 112.9, 113.3, 130.1, 145.0, 156.0, 161.0, 162.5.

7-((10-bromodecyl)oxy)-2H-chromen-2-one (3g). White powder, 65% yield; IR: 3081, 2933, 2916, 2852, 1707, 1617, 1556, 1508, 1472, 1394, 1289, 1234, 1129, 1098, 1034, 1014, 891, 840, 758, 715, 685, 639, 568, 456 cm^{-1} ; ^1H NMR (DMSO- d_6 , 300 MHz) δ/ppm : 1.28–1.36 (14H, m), 1.73–1.80 (4H, m), 3.52 (2H, t, $J = 6.7$ Hz), 4.04–4.08 (2H, m), 6.28 (1H, d, $J = 9.3$ Hz), 6.92–6.98 (2H, m), 7.62 (1H, d, $J = 8.7$ Hz), 7.98 (1H, d, $J = 9.6$ Hz); ^{13}C NMR (DMSO- d_6 , 75 MHz) δ/ppm : 26.1, 29.1, 29.4, 29.6, 29.7, 33.2, 61.3, 68.9, 101.7, 112.9, 113.0, 113.4, 130.1, 145.0, 156.0, 161.0, 162.5.

7-((12-bromododecyl)oxy)-2H-chromen-2-one (3h). White powder, 74% yield; IR: 2934, 2916, 2851, 1720, 1709, 1620, 1556, 1509, 1472, 1395, 1288, 1235, 1130, 1100, 1030, 1007, 891, 825, 745, 716, 640, 616, 569, 457 cm^{-1} ; ^1H NMR (DMSO- d_6 , 300 MHz) δ/ppm : 1.24–1.37 (16H, m), 1.69–1.79 (4H, m), 3.51 (2H, t, $J = 6.4$ Hz), 4.05 (2H, t, $J = 6.1$ Hz), 6.27 (1H, d, $J = 9.3$ Hz), 6.91–6.96 (2H, m), 7.60 (1H, d, $J = 8.4$ Hz), 7.98 (1H, d, $J = 9.6$ Hz); ^{13}C NMR (DMSO- d_6 , 75 MHz) δ/ppm : 26.0, 26.1, 29.0, 29.3, 29.6, 29.7, 33.1, 61.4, 68.9, 101.7, 112.8, 113.0, 113.4, 130.1, 145.1, 156.0, 161.1, 162.5.

4.2.3. General procedure for the of compounds 4a-h

NaN_3 (2 mmol) were added to a solution of **3a-h** (1 mmol) in DMF (15 mL). The reaction was mixture for 8 h at room temperature. The suspension was poured on crushed ice and the precipitated product was filtered and washed with water. It was recrystallized from methanol [39].

7-(2-azidoethoxy)-2H-chromen-2-one (4a). White powder, 97% yield; IR: 3075, 2956, 2160, 2125, 2098, 1726, 1608, 1507, 1406, 1389, 1352, 1279, 1231, 1123, 1053, 994, 914, 892, 835, 750, 616, 550, 522, 460 cm^{-1} ; ^1H NMR (DMSO- d_6 , 300 MHz) δ/ppm : 3.71 (2H, t, $J = 4.6$ Hz), 4.29 (2H, t, $J = 4.3$ Hz), 6.32 (1H, d, $J = 9.3$ Hz), 6.97 (1H, dd, $J = 2.6$ Hz, 8.4 Hz), 7.04 (1H, d, $J = 2.3$ Hz), 7.65 (1H, d,

$J = 8.4$ Hz), 8.02 (1H, d, $J = 9.3$ Hz); ^{13}C NMR (DMSO- d_6 , 75 MHz) δ /ppm: 50.0, 68.1, 101.9, 113.3, 113.4, 130.3, 145.0, 156.0, 160.9, 161.7.

7-(3-azidopropoxy)-2H-chromen-2-one (**4b**). White powder, 98% yield; IR: 3069, 2951, 2882, 2091, 1703, 1612, 1552, 1510, 1400, 1289, 1237, 1129, 1103, 1018, 992, 859, 833, 749, 717, 614, 568, 549, 459 cm^{-1} ; ^1H NMR (DMSO- d_6 , 300 MHz) δ /ppm: 1.94–2.03 (2H, m), 3.50 (2H, t, $J = 6.7$ Hz), 4.12 (2H, t, $J = 6.1$ Hz), 6.26 (1H, dd, $J = 2.0$ Hz, 9.3 Hz), 6.91–6.99 (2H, m), 7.0 (1H, d, $J = 8.4$ Hz), 7.96 (1H, d, $J = 9.6$ Hz); ^{13}C NMR (DMSO- d_6 , 75 MHz) δ /ppm: 28.5, 48.2, 66.1, 101.8, 113.1, 113.2, 113.3, 118.6, 130.1, 145.0, 156.0, 160.9, 162.2, 162.3.

7-(4-azidobutoxy)-2H-chromen-2-one (**4c**). White powder, 46% yield; IR: 3083, 2090, 1719, 1608, 1555, 1507, 1396, 1348, 1281, 1230, 1197, 1121, 992, 830, 751 cm^{-1} ; ^1H NMR (DMSO- d_6 , 300 MHz) δ /ppm: 1.91–2.10 (4H, m), 4.16 (2H, s, br), 6.28 (2H, d, $J = 9.3$ Hz), 6.93–7.0 (2H, m), 7.63 (1H, d, $J = 8.7$ Hz), 8.0 (1H, d, $J = 9.3$ Hz); ^{13}C NMR (DMSO- d_6 , 75 MHz) δ /ppm: 25.7, 51.2, 68.5, 101.8, 112.9, 113.1, 113.4, 130.1, 145.0, 156.0, 161.0, 162.4.

7-((6-azidohexyl)oxy)-2H-chromen-2-one (**4d**). White powder, 62% yield; IR: 3092, 2946, 2930, 2856, 2138, 2088, 1720, 1705, 1608, 1555, 1509, 1473, 1462, 1393, 1295, 1229, 1193, 1128, 1092, 1022, 1001, 846, 751, 723, 615, 569, 478, 461 cm^{-1} ; ^1H NMR (DMSO- d_6 , 300 MHz) δ /ppm: 1.38–1.58 (5H, m), 1.74–1.77 (3H, m), 3.33 (2H, t, $J = 4.3$ Hz), 4.04–4.10 (2H, m), 6.27 (1H, d, $J = 9.3$ Hz), 6.91–6.96 (2H, m), 7.61 (1H, d, $J = 8.4$ Hz), 7.97 (1H, d, $J = 9.3$ Hz); ^{13}C NMR (DMSO- d_6 , 75 MHz) δ /ppm: 25.6, 26.5, 28.8, 29.0, 51.2, 68.8, 101.7, 112.9, 113.0, 113.3, 130.1, 145.0, 156.0, 161.0, 162.5.

7-((7-azidoheptyl)oxy)-2H-chromen-2-one (**4e**). White powder, 80% yield; IR: 3060, 2942, 2097, 1729, 1614, 1555, 1472, 1290, 1239, 1129, 1028, 850, 720 cm^{-1} ; ^1H NMR (DMSO- d_6 , 300 MHz) δ /ppm: 1.29–1.35 (6H, m), 1.46–1.50 (2H, m), 1.65–1.70 (2H, m), 3.26 (2H, t, $J = 6.7$ Hz), 4.00 (2H, t, $J = 6.4$ Hz), 6.24 (1H, d, $J = 9.6$ Hz), 6.86–6.91 (2H, m), 7.56 (1H, d, $J = 8.4$ Hz), 7.93 (1H, d, $J = 9.3$ Hz); ^{13}C NMR (DMSO- d_6 , 75 MHz) δ /ppm: 25.9, 26.7, 28.8, 28.9, 51.2, 68.8, 101.6, 112.8, 112.9, 113.3, 130.1, 145.0, 156.0, 161.0, 162.5.

7-((9-azidononyl)oxy)-2H-chromen-2-one (**4f**). White powder, 86% yield; IR: 3061, 2920, 2096, 1739, 1611, 1556, 1471, 1238, 1097, 1016, 851, 721 cm^{-1} ; ^1H NMR (DMSO- d_6 , 300 MHz) δ /ppm: 1.24–1.36 (10H, m), 1.45–1.49 (2H, m), 1.66–1.68 (2H, m), 3.26 (2H, t, $J = 7.0$ Hz), 4.01 (2H, t, $J = 6.1$ Hz), 6.22 (1H, d, $J = 9.3$ Hz), 6.87–6.92 (2H, m), 7.58 (1H, d, $J = 8.4$ Hz), 7.95 (1H, d, $J = 9.3$ Hz); ^{13}C NMR (DMSO- d_6 , 75 MHz) δ /ppm: 26.0, 26.8, 28.9, 29.0, 29.1, 29.3, 29.5, 51.2, 68.9, 101.6, 112.8, 113.0, 113.3, 130.1, 145.0, 156.0, 161.0, 162.5.

7-((10-azidodecyl)oxy)-2H-chromen-2-one (**4g**). White powder, 78% yield; IR: 3081, 2919, 2852, 2096, 1722, 1709, 1619, 1556, 1508, 1472, 1393, 1378, 1350, 1289, 1236, 1128, 1101, 1018, 890, 829, 758, 746, 631, 616, 569, 456 cm^{-1} ; ^1H NMR (DMSO- d_6 , 300 MHz) δ /ppm: 1.25–1.70 (14H, m), 2.44–2.48 (2H, m), 3.26–3.30 (2H, m), 4.03 (2H, t, $J = 5.5$ Hz), 6.25 (1H, d, $J = 9.3$ Hz), 6.90–6.95 (2H, m), 7.59 (1H, d, $J = 8.4$ Hz), 7.96 (1H, d, $J = 9.3$ Hz); ^{13}C NMR (DMSO- d_6 , 75 MHz) δ /ppm: 26.0, 26.8, 28.9, 29.1, 29.2, 29.3, 29.5, 51.2, 68.9, 101.7, 112.8, 113.0, 113.3, 130.1, 145.0, 156.1, 161.0, 162.5.

7-((12-azidododecyl)oxy)-2H-chromen-2-one (**4h**). White powder, 70% yield; IR: 2917, 2851, 2096, 1722, 1710, 1621, 1557, 1508, 1472, 1393, 1290, 1236, 1130, 1100, 1030, 891, 828, 716, 616, 569, 457 cm^{-1} ; ^1H NMR (DMSO- d_6 , 300 MHz) δ /ppm: 1.25–1.53 (18H, m), 1.67–1.74 (2H, m), 3.30 (2H, t, $J = 6.7$ Hz), 4.06 (2H, t, $J = 6.4$ Hz), 6.27 (1H, d, $J = 9.9$ Hz), 6.91–6.97 (2H, m), 7.62 (1H, d, $J = 8.4$ Hz), 7.98 (1H, d, $J = 9.3$ Hz); ^{13}C NMR (DMSO- d_6 , 75 MHz) δ /ppm: 26.0, 26.8, 28.8, 29.0, 29.1, 29.3, 29.5, 51.2, 68.9, 101.7, 112.8, 113.0, 113.4, 130.1, 145.0, 156.0, 161.0, 162.5.

4.2.4. General procedure for the of compounds 5a-p

2 mmol **4a-h** and 2 mmol **2a-b** were dissolved in a 5 mL of nitrogen-

purged DMF in a Schlenk tube. CuBr (1 mmol) and PMDETA (2 mmol) were added and the reaction mixture was degassed by three cycles and stirred at room temperature for 12 h. After this specified time, the reaction solution was passed through alumina column to remove copper salt and precipitated in water. Next, the crude product was filtered. Finally, the crude product was dried in a vacuum oven at 35 °C [40,41].

7-((1-(2-((2-oxo-2H-chromen-7-yl)oxy)ethyl)-1H-1,2,3-triazol-4-yl)methoxy)-2H-chromen-2-one (**5a**). White powder, 88% yield; mp. 187–189 °C; IR: 3110, 3083, 2954, 1740, 1704, 1607, 1555, 1398, 1228, 1129, 829, 748 cm^{-1} ; ^1H NMR (DMSO- d_6 , 300 MHz) δ /ppm: 4.54 (2H, t, $J = 4.9$ Hz), 4.85 (2H, t, $J = 4.6$ Hz), 5.29 (2H, s), 6.30 (2H, d, $J = 9.3$ Hz), 6.90 (1H, d, $J = 9.8$ Hz), 6.99–7.03 (2H, m), 7.15 (1H, d, $J = 2.0$ Hz), 7.61 (2H, t, $J = 8.4$ Hz), 7.98 (2H, dd, $J = 9.6$, 2.3 Hz), 8.39 (1H, s); ^{13}C NMR (DMSO- d_6 , 75 MHz) δ /ppm: 49.5, 67.4, 79.6, 102.0, 102.1, 102.4, 113.2, 113.3, 113.4, 113.5, 113.6, 126.2, 130.1, 142.6, 144.9X2, 155.9X2, 160.8, 160.9, 161.5, 161.7; LC-MS (m/z): 454 [M^+ + Na]. Anal. Calcd. for $\text{C}_{23}\text{H}_{17}\text{N}_3\text{O}_6$: C, 64.04; H, 3.97; N, 9.74; found: C, 64.06; H, 3.95; N, 9.72.

4-methyl-7-((1-(2-((2-oxo-2H-chromen-7-yl)oxy)ethyl)-1H-1,2,3-triazol-4-yl)methoxy)-2H-chromen-2-one (**5b**). White powder, 92% yield; mp. 192–194 °C; IR: 3200, 3091, 2958, 1706, 1607, 1555, 1398, 1228, 1136, 832, 749 cm^{-1} ; ^1H NMR (DMSO- d_6 , 300 MHz) δ /ppm: 2.39 (3H, s), 4.45 (2H, t, $J = 4.1$ Hz), 4.85 (2H, t, $J = 4.3$ Hz), 5.28 (2H, s), 6.13 (1H, s), 6.27 (1H, d, $J = 9.3$ Hz), 6.76–6.81 (2H, m), 6.89–6.96 (2H, m), 7.38 (1H, d, $J = 8.4$ Hz), 7.50 (1H, d, $J = 8.4$ Hz), 7.63 (1H, d, $J = 8.2$ Hz), 7.88 (1H, s); ^{13}C NMR (DMSO- d_6 , 75 MHz) δ /ppm: 18.9, 49.8, 62.3, 66.9, 101.9, 102.2, 112.4, 112.5, 112.7, 113.5, 114.0, 114.2, 124.4, 125.9, 129.3, 143.4, 152.7, 155.2, 155.8, 160.8, 161.0, 161.2, 161.3; LC-MS (m/z): 468 [M^+ + Na]. Anal. Calcd. for $\text{C}_{24}\text{H}_{19}\text{N}_3\text{O}_6$: C, 64.72; H, 4.30; N, 9.43; found: C, 64.70; H, 4.33; N, 9.44.

7-(3-(4-((2-oxo-2H-chromen-7-yl)oxy)methyl)-1H-1,2,3-triazol-1-yl)propoxy)-2H-chromen-2-one (**5c**). White powder, 94% yield; mp. 150–151 °C; IR: 3120, 3077, 2968, 1723, 1612, 1509, 1298, 1105, 890, 730 cm^{-1} ; ^1H NMR (DMSO- d_6 , 300 MHz) δ /ppm: 2.35–2.50 (2H, m), 4.04 (2H, t, $J = 5.5$ Hz), 4.64 (2H, t, $J = 6.7$ Hz), 5.26 (2H, s), 6.27 (2H, dd, $J = 9.6$, 4.1 Hz), 6.75–6.94 (4H, m), 7.27 (1H, s), 7.38 (2H, d, $J = 8.4$ Hz), 7.64 (1H, d, $J = 9.0$ Hz), 7.69 (1H, s); ^{13}C NMR (DMSO- d_6 , 75 MHz) δ /ppm: 29.8, 47.3, 62.4, 64.8, 101.5, 101.7, 102.2, 112.7, 112.9, 113.1, 113.4, 113.7, 123.6, 129.0, 129.2, 143.3, 143.6, 155.9X2, 161.4, 161.6, 162.1; LC-MS (m/z): 468 [M^+ + Na]. Anal. Calcd. for $\text{C}_{24}\text{H}_{19}\text{N}_3\text{O}_6$: C, 64.72; H, 4.30; N, 9.43; found: C, 64.71; H, 4.32; N, 9.45.

4-methyl-7-((1-(3-((2-oxo-2H-chromen-7-yl)oxy)propyl)-1H-1,2,3-triazol-4-yl)methoxy)-2H-chromen-2-one (**5d**). White powder, 96% yield; mp. 163–164 °C; IR: 3117, 3089, 2983, 1715, 1613, 1458, 1390, 1279, 1200, 1128, 1015, 853, 772 cm^{-1} ; ^1H NMR (DMSO- d_6 , 300 MHz) δ /ppm: 2.29–2.33 (2H, m), 2.48 (3H, m), 4.08 (2H, t, $J = 5.8$ Hz), 4.56 (2H, t, $J = 6.7$ Hz), 5.25 (2H, s), 6.20 (1H, s), 6.28 (2H, d, $J = 9.3$ Hz), 6.85–7.03 (3H, m), 7.12 (1H, d, $J = 2.3$ Hz), 7.60 (1H, t, $J = 4.6$ Hz), 7.67 (1H, d, $J = 8.7$ Hz), 7.97 (1H, d, $J = 9.6$ Hz), 8.33 (1H, s); ^{13}C NMR (DMSO- d_6 , 75 MHz) δ /ppm: 18.8, 29.9, 47.3, 62.3, 66.0, 101.8, 102.1, 111.9, 113.1, 113.3, 114.0, 125.7, 127.1, 130.1, 142.6, 144.9, 154.0, 155.3, 156.0, 160.8, 160.9, 161.6, 162.1, 162.2; LC-MS (m/z): 482 [M^+ + Na]. Anal. Calcd. for $\text{C}_{25}\text{H}_{21}\text{N}_3\text{O}_6$: C, 65.35; H, 4.61; N, 9.15; found: C, 65.33; H, 4.62; N, 9.17.

7-((1-(4-((2-oxo-2H-chromen-7-yl)oxy)butyl)-1H-1,2,3-triazol-4-yl)methoxy)-2H-chromen-2-one (**5e**). White powder, 86% yield; mp. 111–113 °C; IR: 3114, 3082, 2950, 1721, 1708, 1613, 1554, 1394, 1277, 1124, 986, 827 cm^{-1} ; ^1H NMR (DMSO- d_6 , 300 MHz) δ /ppm: 1.69–1.71 (2H, m), 1.95–2.00 (2H, m), 4.07 (2H, t, $J = 6.1$ Hz), 4.45 (2H, t, $J = 6.4$ Hz), 5.24 (2H, s), 6.25–6.29 (2H, m), 6.90–7.01 (3H, m), 7.13 (1H, s), 7.61 (2H, t, $J = 6.7$ Hz), 7.96 (2H, d, $J = 9.3$ Hz), 8.31 (1H, s); ^{13}C NMR (DMSO- d_6 , 75 MHz) δ /ppm: 26.1, 27.1, 49.7, 62.3, 68.2, 101.8, 102.2, 113.0, 113.1, 113.2, 113.4, 113.6, 125.5, 130.2, 142.6, 145.0, 155.9, 156.0, 160.9, 161.0, 161.7, 162.3; LC-MS (m/z):

482 [M⁺ + Na]. Anal.Calcd.for C₂₅H₂₁N₃O₆: C, 65.35; H, 4.61; N, 9.15; found: C, 65.36; H, 4.60; N, 9.16.

4-methyl-7-((1-(4-((2-oxo-2H-chromen-7-yl)oxy)butyl)-1H-1,2,3-triazol-4-yl)methoxy)-2H-chromen-2-one (5f). White powder, 80% yield; mp. 150–151 °C; IR: 3128, 3081, 2959, 1710, 1610, 1511, 1391, 1266, 1126, 989, 826 cm⁻¹; ¹H NMR (DMSO-*d*₆, 300 MHz) δ/ppm: 1.69–1.71 (2H, m), 1.95–1.97 (2H, m), 2.37 (3H, s), 4.07 (2H, t, *J* = 5.5 Hz), 4.45 (2H, t, *J* = 6.7 Hz), 5.25 (2H, s), 6.20 (1H, s), 6.26 (1H, d, *J* = 9.3 Hz), 6.89–7.02 (3H, m), 7.12 (1H, s), 7.60 (1H, d, *J* = 8.2 Hz), 7.67 (1H, d, *J* = 8.7 Hz), 7.96 (1H, d, *J* = 9.3 Hz), 8.31 (1H, s); ¹³C NMR (DMSO-*d*₆, 75 MHz) δ/ppm: 18.8, 26.1, 27.1, 49.7, 62.3, 68.2, 101.8, 102.2, 111.9, 113.0, 113.1, 113.3, 113.4, 114.0, 125.5, 127.1, 130.1, 142.6, 145.0, 154.1, 155.3, 156.0, 160.8, 161.0, 161.7, 162.3; LC-MS (*m/z*): 496 [M⁺ + Na]. Anal.Calcd.for C₂₆H₂₃N₃O₆: C, 65.95; H, 4.90; N, 8.87; found: C, 65.97; H, 4.92; N, 8.85.

7-((1-(6-((2-oxo-2H-chromen-7-yl)oxy)hexyl)-1H-1,2,3-triazol-4-yl)methoxy)-2H-chromen-2-one (5g). White powder, 74% yield; mp. 111–112 °C; IR: 3129, 3083, 2942, 1731, 1615, 1506, 1398, 1274, 1126, 985, 850 cm⁻¹; ¹H NMR (DMSO-*d*₆, 300 MHz) δ/ppm: 1.29–1.31 (2H, m), 1.41–1.46 (2H, m), 1.68–1.73 (2H, m), 1.83–1.87 (2H, m), 4.04 (2H, t, *J* = 6.4 Hz), 4.39 (2H, t, *J* = 7.0 Hz), 5.26 (2H, s), 6.29 (2H, t, *J* = 7.6 Hz), 6.90–6.96 (2H, m), 7.00 (1H, d, *J* = 8.4 Hz), 7.14 (1H, d, *J* = 2.3 Hz), 7.62 (2H, t, *J* = 7.0 Hz), 7.98 (1H, dd, *J* = 9.6, 3.8 Hz), 8.30 (1H, s); ¹³C NMR (DMSO-*d*₆, 75 MHz) δ/ppm: 25.4, 26.1, 28.8, 30.2, 50.0, 62.3, 68.2, 101.7, 102.2, 112.9, 113.0, 113.2, 113.3, 113.6, 125.4, 130.1X2, 142.5, 144.9, 145.0, 155.9, 156.0, 160.9, 161.0, 161.7, 162.5; LC-MS (*m/z*): 510 [M⁺ + Na]. Anal.Calcd.for C₂₇H₂₅N₃O₆: C, 66.52; H, 5.17; N, 8.62; found: C, 66.50; H, 5.18; N, 8.63.

4-methyl-7-((1-(6-((2-oxo-2H-chromen-7-yl)oxy)hexyl)-1H-1,2,3-triazol-4-yl)methoxy)-2H-chromen-2-one (5h). White powder, 72% yield; mp. 108–110 °C; IR: 3120, 3069, 2936, 1710, 1609, 1556, 1390, 1267, 1123, 990, 874 cm⁻¹; ¹H NMR (DMSO-*d*₆, 300 MHz) δ/ppm: 1.29–1.36 (2H, m), 1.39–1.48 (2H, m), 1.68–1.75 (2H, m), 1.81–1.88 (2H, m), 2.39 (3H, s), 4.03 (2H, t, *J* = 6.1 Hz), 4.39 (2H, t, *J* = 7.0 Hz), 5.26 (2H, s), 6.21 (1H, s), 6.27 (1H, d, *J* = 9.3 Hz), 6.90–6.95 (2H, m), 7.01 (1H, dd, *J* = 8.7, 2.6 Hz), 7.12 (1H, d, *J* = 2.3 Hz), 7.60 (1H, d, *J* = 8.4 Hz), 7.67 (1H, d, *J* = 8.7 Hz), 7.97 (1H, d, *J* = 9.3 Hz), 8.30 (1H, s); ¹³C NMR (DMSO-*d*₆, 75 MHz) δ/ppm: 18.7, 25.4, 26.1, 28.8, 30.2, 50.0, 62.3, 68.8, 101.7, 102.2, 111.9, 112.9, 113.0, 113.2, 113.3, 114.0, 125.4, 127.1, 130.1, 142.5, 144.9, 154.0, 155.3, 156.0, 160.7, 160.9, 161.6, 162.5; LC-MS (*m/z*): 524 [M⁺ + Na]. Anal.Calcd.for C₂₈H₂₇N₃O₆: C, 67.05; H, 5.43; N, 8.38; found: C, 67.07; H, 5.41; N, 8.36.

7-((1-(7-((2-oxo-2H-chromen-7-yl)oxy)heptyl)-1H-1,2,3-triazol-4-yl)methoxy)-2H-chromen-2-one (5i). White powder, 74% yield; mp. 106–107 °C; IR: 3127, 3083, 2943, 1726, 1617, 1506, 1275, 1160, 1126, 850, 822 cm⁻¹; ¹H NMR (DMSO-*d*₆, 300 MHz) δ/ppm: 1.23–1.36 (6H, m), 1.68–1.70 (2H, m), 1.80–1.85 (2H, m), 4.04 (2H, t, *J* = 6.4 Hz), 4.38 (2H, t, *J* = 7.0 Hz), 5.26 (2H, s), 6.26–6.32 (2H, m), 6.91–7.03 (3H, m), 7.15 (1H, s), 7.62 (2H, t, *J* = 7.6 Hz), 7.99 (2H, dd, *J* = 9.6, 3.2 Hz), 8.29 (1H, s); ¹³C NMR (DMSO-*d*₆, 75 MHz) δ/ppm: 25.9, 26.4, 28.6, 28.9, 30.2, 50.0, 62.3, 68.8, 101.7, 102.1, 112.2, 113.0, 113.2, 113.4, 113.6, 125.4, 130.1, 142.4, 145.0, 155.9, 156.0, 161.0, 161.7, 162.5; LC-MS (*m/z*): 524 [M⁺ + Na]. Anal.Calcd.for C₂₈H₂₇N₃O₆: C, 67.05; H, 5.43; N, 8.38; found: C, 67.04; H, 5.42; N, 8.39.

4-methyl-7-((1-(7-((2-oxo-2H-chromen-7-yl)oxy)heptyl)-1H-1,2,3-triazol-4-yl)methoxy)-2H-chromen-2-one (5j). White powder, 68% yield; mp. 102–104 °C; IR: 3127, 3083, 2943, 1726, 1614, 1506, 1345, 1275, 1160, 1126, 985, 822 cm⁻¹; ¹H NMR (DMSO-*d*₆, 300 MHz) δ/ppm: 1.21–1.42 (6H, m), 1.77–1.81 (2H, m), 1.94–1.98 (2H, m), 2.37 (3H, s), 3.98 (2H, t, *J* = 6.4 Hz), 4.42 (2H, t, *J* = 7.0 Hz), 5.24 (2H, s), 6.10 (1H, s), 6.22 (1H, d, *J* = 9.3 Hz), 6.72 (1H, s), 6.80–6.95 (2H, m), 7.36–7.38 (2H, m), 7.48 (1H, d, *J* = 8.7 Hz), 7.65 (1H, d, *J* = 9.3 Hz), 7.81 (1H, s); ¹³C NMR (DMSO-*d*₆, 75 MHz) δ/ppm: 18.8, 25.9, 26.5,

28.8, 28.9, 30.3, 50.5, 62.3, 68.5, 101.3, 102.0, 112.1, 112.5, 112.6, 112.8, 112.9, 114.0, 123.4, 125.9, 129.0, 142.9, 143.8, 152.8, 155.1, 155.9, 161.2, 161.3, 161.4, 162.4; LC-MS (*m/z*): 538 [M⁺ + Na]. Anal.Calcd.for C₂₉H₂₉N₃O₆: C, 67.56; H, 5.67; N, 8.15; found: C, 67.55; H, 5.68; N, 8.14.

7-((9-((4-((2-oxo-2H-chromen-7-yl)oxy)methyl)-1H-1,2,3-triazol-1-yl)nonyl)oxy)-2H-chromen-2-one (5k). White powder, 78% yield; mp. 108–109 °C; IR: 3127, 3083, 2919, 1729, 1614, 1506, 1399, 1274, 1126, 995, 854 cm⁻¹; ¹H NMR (DMSO-*d*₆, 300 MHz) δ/ppm: 1.15–1.32 (10H, m), 1.68–1.80 (4H, m), 4.03 (2H, t, *J* = 3.22 Hz), 4.33 (2H, t, *J* = 7.0 Hz), 5.23 (2H, s), 6.26 (2H, q, *J* = 7.6 Hz), 6.84–7.00 (3H, m), 7.11 (1H, t, *J* = 2.3 Hz), 7.59 (2H, t, *J* = 7.6 Hz), 7.95 (2H, dd, *J* = 9.3, 3.5 Hz), 8.26 (1H, s); ¹³C NMR (DMSO-*d*₆, 75 MHz) δ/ppm: 26.0, 26.4, 28.9, 29.4, 30.3, 31.0, 50.0, 62.3, 68.9, 101.7, 102.2, 112.8, 113.0, 113.2, 113.3, 113.6, 125.4, 130.1, 142.5, 145.0, 155.9, 156.0, 160.9, 161.0, 161.7, 162.5; LC-MS (*m/z*): 552 [M⁺ + Na]. Anal.Calcd.for C₃₀H₃₁N₃O₆: C, 68.04; H, 5.90; N, 7.93; found: C, 68.06; H, 5.91; N, 7.90.

4-methyl-7-((1-(9-((2-oxo-2H-chromen-7-yl)oxy)nonyl)-1H-1,2,3-triazol-4-yl)methoxy)-2H-chromen-2-one (5l). White powder, 76% yield; mp. 118–119 °C; IR: 3127, 3078, 2931, 1713, 1611, 1555, 1388, 1282, 1125, 825 cm⁻¹; ¹H NMR (DMSO-*d*₆, 300 MHz) δ/ppm: 1.25–1.38 (10H, m), 1.68–1.83 (4H, m), 2.39 (3H, s), 4.04 (2H, t, *J* = 6.4 Hz), 4.37 (2H, t, *J* = 6.7 Hz), 5.26 (2H, s), 6.22 (1H, s), 6.27 (1H, d, *J* = 9.3 Hz), 6.91–7.04 (3H, m), 7.13 (1H, d, *J* = 2.3 Hz), 7.60 (1H, d, *J* = 8.4 Hz), 7.68 (1H, d, *J* = 8.7 Hz), 7.98 (1H, d, *J* = 9.3 Hz), 8.29 (1H, s); ¹³C NMR (DMSO-*d*₆, 75 MHz) δ/ppm: 18.8, 26.0, 26.4, 28.9, 29.0, 29.2, 29.4, 30.3, 50.0, 62.3, 68.9, 101.7, 102.2, 111.9, 112.8, 113.0, 113.2, 113.3, 113.9, 125.4, 127.1, 130.1, 142.5, 145.0, 154.0, 155.3, 156.0, 160.8, 161.0, 161.6, 162.5; LC-MS (*m/z*): 566 [M⁺ + Na]. Anal.Calcd.for C₃₁H₃₃N₃O₆: C, 68.49; H, 6.12; N, 7.73; found: C, 68.47; H, 6.10; N, 7.75.

7-((1-(10-((2-oxo-2H-chromen-7-yl)oxy)decyl)-1H-1,2,3-triazol-4-yl)methoxy)-2H-chromen-2-one (5m). White powder, 82% yield; mp. 115–116 °C; IR: 3129, 3083, 2920, 1731, 1615, 1506, 1399, 1276, 1098, 985, 850 cm⁻¹; ¹H NMR (DMSO-*d*₆, 300 MHz) δ/ppm: 1.20–1.35 (12H, m), 1.66–1.79 (4H, m), 4.01 (2H, t, *J* = 6.1 Hz), 4.33 (2H, t, *J* = 7.0 Hz), 5.23 (2H, s), 6.23–6.29 (2H, m), 6.87–7.00 (3H, m), 7.11 (1H, d, *J* = 2.3 Hz), 7.56–7.61 (2H, m), 7.95 (2H, dd, *J* = 9.6, 3.2 Hz), 8.26 (1H, s); ¹³C NMR (DMSO-*d*₆, 75 MHz) δ/ppm: 26.0, 26.4, 29.0, 29.1, 29.3, 29.4, 29.5, 30.3, 50.0, 62.3, 68.9, 101.7, 102.1, 112.8, 113.0, 113.2, 113.3, 113.6, 125.4, 130.1, 142.5, 144.9, 145.0, 155.9, 156.0, 160.9, 161.0, 161.7, 162.5; LC-MS (*m/z*): 566 [M⁺ + Na]. Anal.Calcd.for C₃₁H₃₃N₃O₆: C, 68.49; H, 6.12; N, 7.73; found: C, 68.48; H, 6.11; N, 7.76.

4-methyl-7-((1-(10-((2-oxo-2H-chromen-7-yl)oxy)decyl)-1H-1,2,3-triazol-4-yl)methoxy)-2H-chromen-2-one (5n). White powder, 84% yield; mp. 106–107 °C; IR: 3150, 3083, 2917, 1727, 1618, 1554, 1387, 1298, 1134, 998, 836 cm⁻¹; ¹H NMR (CDCl₃, 300 MHz) δ/ppm: 1.26–1.46 (12H, m), 1.60–1.61 (2H, m), 1.78–1.93 (2H, m), 2.40 (3H, s), 4.01 (2H, t, *J* = 6.4 Hz), 4.38 (2H, t, *J* = 7.3 Hz), 5.27 (2H, s), 6.16 (1H, s), 6.25 (1H, d, *J* = 9.6 Hz), 6.79–6.85 (2H, m), 6.93–6.98 (2H, m), 7.36 (1H, d, *J* = 8.7 Hz), 7.51 (1H, d, *J* = 8.7 Hz), 7.63–7.66 (2H, m); ¹³C NMR (CDCl₃, 75 MHz) δ/ppm: 18.9, 26.1, 26.6, 29.1, 29.4, 29.5, 30.5, 50.7, 62.5, 68.8, 101.4, 102.3, 112.5, 112.6, 113.1, 113.2, 114.2, 122.9, 125.9, 128.9, 143.1, 143.7, 152.7, 155.3, 156.1, 161.3, 162.6; LC-MS (*m/z*): 580 [M⁺ + Na]. Anal.Calcd.for C₃₂H₃₅N₃O₆: C, 68.92; H, 6.33; N, 7.54; found: C, 68.93; H, 6.35; N, 7.51.

7-((1-(12-((2-oxo-2H-chromen-7-yl)oxy)dodecyl)-1H-1,2,3-triazol-4-yl)methoxy)-2H-chromen-2-one (5o). White powder, 85% yield; mp. 116–117 °C; IR: 3129, 3087, 2918, 1730, 1615, 1507, 1397, 1232, 1126, 987, 822 cm⁻¹; ¹H NMR (DMSO-*d*₆, 300 MHz) δ/ppm: 1.16–1.35 (16H, m), 1.65–1.78 (4H, m), 4.01 (2H, t, *J* = 6.1 Hz), 4.33 (2H, t, *J* = 7.0 Hz), 5.23 (2H, s), 6.25 (2H, t, *J* = 9.3 Hz), 6.86–6.99 (3H, m), 7.11 (1H, d, *J* = 2.0 Hz), 7.58 (2H, t, *J* = 8.4 Hz), 7.95 (2H, dd, *J* = 9.3, 3.8 Hz), 8.26 (1H, s); ¹³C NMR (DMSO-*d*₆, 75 MHz) δ/ppm: 26.1, 26.4,

29.0, 29.1, 29.4, 29.5, 29.6, 30.3, 50.0, 62.3, 68.9, 101.7, 102.1, 112.8, 113.0, 113.2, 113.3, 113.6, 125.4, 130.1, 142.5, 145.0, 155.9, 156.0, 160.9, 161.0, 161.7, 162.5; LC-MS (*m/z*): 594 [$M^+ + Na$]. Anal.Calcd.for $C_{33}H_{37}N_3O_6$: C, 69.33; H, 6.52; N, 7.35; found: C, 69.35; H, 6.51; N, 7.34.

4-methyl-7-((1-(12-((2-oxo-2H-chromen-7-yl)oxy)dodecyl)-1H-1,2,3-triazol-4-yl)methoxy)-2H-chromen-2-one (**5p**). White powder, 84% yield; mp. 103–105 °C; IR: 3134, 3083, 2917, 1726, 1614, 1508, 1389, 1276, 1129, 836 cm^{-1} ; 1H NMR (DMSO- d_6 , 300 MHz) δ /ppm: 1.18–1.37 (16H, m), 1.67–1.79 (4H, m), 2.37 (3H, s), 4.02 (2H, t, $J = 6.4$ Hz), 4.33 (2H, t, $J = 7.0$ Hz), 5.24 (2H, s), 6.19 (1H, s), 6.25 (1H, d, $J = 9.3$ Hz), 6.88–7.02 (2H, m), 7.11 (1H, d, $J = 2.3$ Hz), 7.57 (1H, d, $J = 8.4$ Hz), 7.65 (1H, d, $J = 8.7$ Hz), 7.95 (2H, d, $J = 9.6$ Hz), 8.25 (1H, s); ^{13}C NMR (DMSO- d_6 , 75 MHz) δ /ppm: 18.8, 26.0, 26.4, 29.0, 29.1, 29.3, 29.5, 29.6, 30.3, 50.0, 62.3, 68.9, 101.7, 102.1, 111.9, 112.8, 113.0, 113.3, 113.4, 114.0, 125.4, 127.1, 130.1, 142.5, 145.0, 154.0, 155.3, 156.0, 160.8, 161.0, 161.6, 162.5; LC-MS (*m/z*): 586 [M^+]. Anal.Calcd.for $C_{34}H_{39}N_3O_6$: C, 69.72; H, 6.71; N, 7.17; found: C, 69.74; H, 6.72; N, 7.15.

4.3. CA inhibition assays

An SX.18 V-R Applied Photophysics (Oxford, UK) stopped flow instrument has been used to assay the catalytic/inhibition of various CA isozymes [42]. Phenol Red (at a concentration of 0.2 mM) has been used as an indicator, working at an absorbance maximum of 557 nm, with 10 mM Hepes (pH 7.4) as a buffer, 0.1 M Na_2SO_4 or $NaClO_4$ (for maintaining constant the ionic strength; these anions are not inhibitory in the used concentration), following the CA-catalyzed CO_2 hydration reaction for a period of 5–10 s. Saturated CO_2 solutions in water at 25 °C were used as substrate. Stock solutions of inhibitors were prepared at a concentration of 10 mM (in DMSO-water 1:1, v/v) and dilutions up to 0.01 nM done with the assay buffer mentioned above. At least 7 different inhibitor concentrations have been used for measuring the inhibition constant. Inhibitor and enzyme solutions were pre-incubated together for 6 h at 4 °C prior to assay, in order to allow for the formation of the E-I complex. Triplicate experiments were done for each inhibitor concentration, and the values reported in this paper are the mean of such results. The inhibition constants were obtained by non-linear least squares methods using the Cheng-Prusoff equation, as reported earlier, and represent the mean from at least three different determinations [43]. All CA isozymes used here were recombinant proteins obtained as reported earlier by our group [43–45].

4.4. Molecular modeling

Although there are some crystal structures of hCA IX and XII already deposited on protein data bank (PDB) server, these structures are co-crystallized with sulfonamide CA inhibitors or apo form (for isoform IX). However, coumarin derivatives were shown to plug the entrance to the enzyme active site and make no interactions with Zn^{++} ion [30,31,46]. Hence target binding site of studied compounds were expected to be different than the ones of the crystal structures with sulfonamide CA inhibitors. Therefore, the crystal structures with PDB codes 5DVX [47] and 5MSA [48] for hCA IX and XII were retrieved, respectively. The crystal structure of coumarin derivative bound hCA II that was resolved by Maresca et al. with PDB code 3F8E was also downloaded [30]. Firstly, the mutated sequences in crystal structure (if there was any) were corrected to match the wild type sequences in UniProt. The crystal structures were prepared using Protein Preparation Wizard [49] implemented in the Schrodinger package with the default settings. The ions, small molecules such as some derivatives of glycol that were used to help crystallization and all but Zn^{++} ion coordinated water molecules were removed. Protonation states of amino acids were predicted using PROPKA [50] whereas Epik [51] was used to predict ionization and tautomeric states of the co-crystallized ligand at the

physiological pH of 7.4. Restraint geometry optimization and energy minimization with OPLS3 forcefield was the last step of protein preparation [52]. To correctly assess the binding pocket of coumarins and hence the studied compounds for isoforms IX and XII, the prepared hCA IX and hCA XII isoform structures were aligned to prepared hCA II – coumarin derivative structures. Then, the co-crystallized ligands inside isoforms hCA IX and XII were removed. The coumarin derivative of hCA II isoform as well as Zn^{++} -coordinated water molecule was inserted into prepared hCA IX and XII isoform structures. Maestro modeling package was used to visualize and alignment of structures [53]. As there may be some clashes in obtained complex structures, molecular dynamics (MD) simulations were performed to adjust specifically side chains of coumarin binding site. The complexes were placed in orthorhombic boxes of TIP3P water molecules with box sizes of 10 Å along all three dimensions. The systems were all neutralized and ionic concentration of 0.15 M NaCl solution was used to adjust concentration of the solvent systems. The Desmond all atom MD simulations program was used [54]. Default settings of Desmond package with temperature of 310 K were used along with default relaxation protocol. MD simulations were performed for 10 ns. Then, the trajectories obtained by simulations were clustered based on the average RMSD differences of ligand molecule. The representative structure from the cluster with the largest size was taken as initial complex structure for docking studies.

As mentioned before, coumarin derivatives could hydrolyze to form cinnamic acid derivatives [31]. Since there are two coumarin rings in the studied molecules as shown in Fig. 1, three different hydrolysis products could be formed. The structures of studied compounds along with their three possible hydrolysis products were drawn using Maestro and 3D structures were first subjected to restrained minimization. Then, LigPrep module [55] of Schrodinger with OPLS3 forcefield were used to prepare the compounds. The Schrodinger Epik module was used to generate ionization for molecules at pH 7.4.

Molecular docking studies were performed by GOLD docking program [56–58] that is based on a genetic algorithm for docking flexible ligands into binding sites. Here, representative structures of largest cluster of MD trajectories were used as protein-ligand complexed. The binding site was shaped residues within 6 Å vicinity of ligands in complexes. While proteins binding pocket were held rigid during docking, side chains of some amino acid such as Serine, Threonine and Tyrosine hydroxyl groups and Lysine NH_3^+ groups were optimized (i.e., rotamers of these residues were considered) throughout the docking in order to maximize the flexibility of binding pocket residues. For ligand flexibility the default settings were considered, however protonated carboxylic acid groups and ring-NHR or ring-NR1R2 groups were rotated instead of flipped. 50 docking poses were requested for each ligand and to increase the accuracy of binding pose prediction, diverse solutions options with cluster size of 5 and RMSD differences of 3 Å were chosen. Default settings were used for population (population size, 100) and genetic operations (number of operations, 10000) steps. Search efficiency were set as 200% as recommended for large highly flexible ligands. CHEMPLP fitness function of GOLD package was used for pose prediction as it was found to give the highest success rates for pose prediction and virtual screening experiments against diverse test sets and the default function of GOLD.

Acknowledgments

This work was supported by the Bezmialem Research Fund of the Bezmialem Vakif University. Project Number: 6.2016/11.

Appendix A. Supplementary material

Supplementary data to this article can be found online at <https://doi.org/10.1016/j.bioorg.2019.03.003>.

References

- [1] A. Karioti, M. Ceruso, F. Carta, A.R. Bilia, C.T. Supuran, New natural product carbonic anhydrase inhibitors incorporating phenol moieties, *Bioorg. Med. Chem.* 23 (22) (2015) 7219–7225.
- [2] C.T. Supuran, Carbonic anhydrases: novel therapeutic applications for inhibitors and activators, *Nat. Rev. Drug Discov.* 7 (2) (2008) 168–181.
- [3] Y. Le Duc, E. Licsandru, D. Vullo, M. Barboiu, C.T. Supuran, Carbonic anhydrases activation with 3-amino-1H-1,2,4-triazole-1-carboxamides: discovery of subnanomolar isoform II activators, *Bioorg. Med. Chem.* 25 (5) (2017) 1681–1686.
- [4] C.T. Supuran, Carbonic anhydrase inhibitors, *Bioorg. Med. Chem. Lett.* 20 (12) (2010) 3467–3474.
- [5] A. Angeli, A.A.M. Abdel-Aziz, A. Nocentini, A.S. El-Azab, P. Gratteri, C.T. Supuran, Synthesis and carbonic anhydrase inhibition of polycyclic imides incorporating N-benzenesulfonamide moieties, *Bioorg. Med. Chem.* 25 (20) (2017) 5373–5379.
- [6] M. Ferraroni, F. Carta, A. Scozzafava, C.T. Supuran, Thioxocoumarins show an alternative carbonic anhydrase inhibition mechanism compared to coumarins, *J. Med. Chem.* 59 (1) (2016) 462–473.
- [7] S. Akocak, N. Lolak, A. Nocentini, G. Karakoc, A. Tufan, C.T. Supuran, Synthesis and biological evaluation of novel aromatic and heterocyclic bis-sulfonamide Schiff bases as carbonic anhydrase I, II, VII and IX inhibitors, *Bioorg. Med. Chem.* 25 (12) (2017) 3093–3097.
- [8] A. Grandane, M. Tanc, L. Di Cesare Mannelli, F. Carta, C. Ghelardini, R. Zalubovskis, C.T. Supuran, 6-Substituted sulfocoumarins are selective carbonic anhydrase IX and XII inhibitors with significant cytotoxicity against colorectal cancer cells, *J. Med. Chem.* 58 (9) (2015) 3975–3983.
- [9] A. Bonardi, M. Falsini, D. Catarzi, F. Varano, L.D. Mannelli, B. Tenci, C. Ghelardini, A. Angeli, C.T. Supuran, V. Colotta, Structural investigations on coumarins leading to chromeno[4,3-c]pyrazol-4-ones and pyrano[4,3-c]pyrazol-4-ones: New scaffolds for the design of the tumor-associated carbonic anhydrase isoforms IX and XII, *Eur. J. Med. Chem.* 146 (2018) 47–59.
- [10] A. Nocentini, F. Carta, M. Ceruso, G. Bartolucci, C.T. Supuran, Click-tailed coumarins with potent and selective inhibitory action against the tumor-associated carbonic anhydrases IX and XII, *Bioorg. Med. Chem.* 23 (21) (2015) 6955–6966.
- [11] L. De Luca, F. Mancuso, S. Ferro, M.R. Buemi, A. Angeli, S. Del Prete, C. Capasso, C.T. Supuran, R. Gitto, Inhibitory effects and structural insights for a novel series of coumarin-based compounds that selectively target human CA IX and CA XII carbonic anhydrases, *Eur. J. Med. Chem.* 143 (2018) 276–282.
- [12] M. Bozdog, A.M. Alafeefy, A.M. Altamimi, D. Vullo, F. Carta, C.T. Supuran, Coumarins and other fused bicyclic heterocycles with selective tumor-associated carbonic anhydrase isoforms inhibitory activity, *Bioorg. Med. Chem.* 25 (2) (2017) 677–683.
- [13] S. Angapelly, P.V.S. Ramya, A. Angeli, C.T. Supuran, M. Arifuddin, Sulfocoumarin-coumarin-, 4-sulfamoylphenyl-bearing indazole-3-carboxamide hybrids: synthesis and selective inhibition of tumor-associated carbonic anhydrase isozymes IX and XII, *ChemMedChem* 12 (19) (2017) 1578–1584.
- [14] K. Tars, D. Vullo, A. Kazaks, J. Leitans, A. Lends, A. Grandane, R. Zalubovskis, A. Scozzafava, C.T. Supuran, Sulfocoumarins (1,2-Benzoxathiine-2,2-dioxides): a class of potent and isoform-selective inhibitors of tumor-associated carbonic anhydrases, *J. Med. Chem.* 56 (1) (2013) 293–300.
- [15] A. Grandane, M. Tanc, R. Zalubovskis, C.T. Supuran, Synthesis of 6-aryl-substituted sulfocoumarins and investigation of their carbonic anhydrase inhibitory action, *Bioorg. Med. Chem.* 23 (7) (2015) 1430–1436.
- [16] N. Chandak, M. Ceruso, C.T. Supuran, P.K. Sharma, Novel sulfonamide bearing coumarin scaffolds as selective inhibitors of tumor associated carbonic anhydrase isoforms IX and XII, *Bioorg. Med. Chem.* 24 (13) (2016) 2882–2886.
- [17] S.D. Lee, W. Kim, J.W. Jeong, J.W. Park, J.E. Kim, AK-1, a SIRT2 inhibitor, destabilizes HIF-1 alpha and diminishes its transcriptional activity during hypoxia, *Cancer Lett.* 373 (1) (2016) 138–145.
- [18] A. Thiry, J.M. Dogne, B. Masereel, C.T. Supuran, Targeting tumor-associated carbonic anhydrase IX in cancer therapy, *Trends Pharmacol. Sci.* 27 (11) (2006) 566–573.
- [19] J. Pastorek, S. Pastorekova, Hypoxia-induced carbonic anhydrase IX as a target for cancer therapy: from biology to clinical use, *Semin. Cancer Biol.* 31 (2015) 52–64.
- [20] L.H. Wang, X.R. Jiang, J.Y. Yang, X.F. Bao, J.L. Chen, X. Liu, G.L. Chen, C.F. Wu, SYP-5, a novel HIF-1 inhibitor, suppresses tumor cells invasion and angiogenesis, *Eur. J. Pharmacol.* 791 (2016) 560–568.
- [21] C.T. Supuran, V. Alterio, A. Di Fiore, K. D. A., F. Carta, S.M. Monti, G. De Simone, Inhibition of carbonic anhydrase IX targets primary tumors, metastases, and cancer stem cells: three for the price of one. *Med. Res. Rev.*, 2018.
- [22] M. Takacova, P. Bullova, V. Simko, L. Skvarkova, M. Poturnajova, L. Feketeova, P. Babal, A.J. Kivela, T. Kuopio, J. Kopacek, J. Pastorek, S. Parkkila, S. Pastorekova, Expression pattern of carbonic anhydrase IX in Medullary thyroid carcinoma supports a role for RET-mediated activation of the HIF pathway, *Am. J. Pathol.* 184 (4) (2014) 953–965.
- [23] K. Horie, K. Kawakami, Y. Fujita, M. Sugaya, K. Kameyama, K. Mizutani, T. Deguchi, M. Ito, Exosomes expressing carbonic anhydrase 9 promote angiogenesis, *Biochem. Biophys. Res. Commun.* 492 (3) (2017) 356–361.
- [24] P.H. Maxwell, M.S. Wiesener, G.W. Chang, S.C. Clifford, E.C. Vaux, M.E. Cockman, C.C. Wykoff, C.W. Pugh, E.R. Maher, P.J. Ratcliffe, The tumour suppressor protein VHL targets hypoxia-inducible factors for oxygen-dependent proteolysis, *Nature* 399 (6733) (1999) 271–275.
- [25] J. Peerlings, L. Van De Voorde, C. Mitea, R. Larue, A. Yaromina, S. Sandeleanu, L. Spiegelberg, L. Dubois, P. Lambin, F.M. Mortaghy, Hypoxia and hypoxia response-associated molecular markers in esophageal cancer: a systematic review, *Methods* 130 (2017) 51–62.
- [26] A. Mollica, R. Costante, A. Akdemir, S. Carradori, A. Stefanucci, G. Macedonio, M. Ceruso, C.T. Supuran, Exploring new Probenecid-based carbonic anhydrase inhibitors: synthesis, biological evaluation and docking studies, *Bioorg. Med. Chem. Lett.* 23 (17) (2015) 5311–5318.
- [27] M. D'Ascenzio, P. Guglielmi, S. Carradori, D. Secci, R. Florio, A. Mollica, M. Ceruso, A. Akdemir, A.P. Sobolev, C.T. Supuran, Open saccharin-based secondary sulfonamides as potent and selective inhibitors of cancer-related carbonic anhydrase IX and XII isoforms, *J. Enzyme Inhib. Med. Chem.* 32 (1) (2017) 51–59.
- [28] A. Mollica, G. Macedonio, A. Stefanucci, S. Carradori, A. Akdemir, A. Angeli, C.T. Supuran, Five- and six-membered nitrogen-containing compounds as selective carbonic anhydrase activators. *Molecules*, 2017, vol. 22, 12 pii: E2178. 10.3390/molecules22122178.
- [29] A. Stefanucci, A. Angeli, M.P. Dimmito, G. Luisi, S. Del Prete, C. Capasso, W.A. Donald, A. Mollica, C.T. Supuran, Activation of beta- and gamma-carbonic anhydrases from pathogenic bacteria with tripeptides, *J. Enzyme Inhib. Med. Chem.* 33 (1) (2018) 945–950.
- [30] A. Maresca, C. Temperini, H. Vu, N.B. Pham, S.A. Poulsen, A. Scozzafava, R.J. Quinn, C.T. Supuran, Non-zinc mediated inhibition of carbonic anhydrases: coumarins are a new class of suicide inhibitors, *J. Am. Chem. Soc.* 131 (8) (2009) 3057–3062.
- [31] A. Maresca, C. Temperini, L. Pochet, B. Masereel, A. Scozzafava, C.T. Supuran, Deciphering the mechanism of carbonic anhydrase inhibition with coumarins and thiocoumarins, *J. Med. Chem.* 53 (1) (2010) 335–344.
- [32] A. Maresca, A. Scozzafava, C.T. Supuran, 7,8-Disubstituted- but not 6,7-disubstituted coumarins selectively inhibit the transmembrane, tumor-associated carbonic anhydrase isoforms IX and XII over the cytosolic ones I and II in the low nanomolar/subnanomolar range, *Bioorg. Med. Chem. Lett.* 20 (24) (2010) 7255–7258.
- [33] J. Wagner, B.S. Avvaru, A.H. Robbins, A. Scozzafava, C.T. Supuran, R. McKenna, Coumarinyl-substituted sulfonamides strongly inhibit several human carbonic anhydrase isoforms: solution and crystallographic investigations, *Bioorg. Med. Chem.* 18 (14) (2010) 4873–4878.
- [34] B.Z. Kurt, F. Sonmez, S. Durdagi, B. Aksoydan, R.E. Salmas, A. Angeli, M. Kucukislamoglu, C.T. Supuran, Synthesis, biological activity and multiscale molecular modeling studies for coumarin-carboxamide derivatives as selective carbonic anhydrase IX inhibitors, *J. Enzyme Inhib. Med. Chem.* 32 (1) (2017) 1042–1052.
- [35] M. Tanc, F. Carta, M. Bozdog, A. Scozzafava, C.T. Supuran, 7-Substituted-sulfocoumarins are isoform-selective, potent carbonic anhydrase II inhibitors, *Bioorg. Med. Chem.* 21 (15) (2013) 4502–4510.
- [36] A. Maresca, C.T. Supuran, Coumarins incorporating hydroxy- and chloro-moieties selectively inhibit the transmembrane, tumor-associated carbonic anhydrase isoforms IX and XII over the cytosolic ones I and II, *Bioorg. Med. Chem. Lett.* 20 (15) (2010) 4511–4514.
- [37] S. Montanari, L. Scalvini, M. Bartolini, F. Belluti, S. Gobbi, V. Andrisano, A. Ligresti, V. Di Marzo, S. Rivara, M. Mor, A. Bisi, A. Rampa, Fatty Acid Amide Hydrolase (FAAH), Acetylcholinesterase (AChE), and Butyrylcholinesterase (BuChE): networked targets for the development of carbamates as potential anti-Alzheimer's disease agents, *J. Med. Chem.* 59 (13) (2016) 6387–6406.
- [38] Y.C. Duan, Y.C. Ma, E. Zhang, X.J. Shi, M.M. Wang, X.W. Ye, H.M. Liu, Design and synthesis of novel 1,2,3-triazole-dithiocarbamate hybrids as potential anticancer agents, *Eur. J. Med. Chem.* 62 (2013) 11–19.
- [39] M.R.J. Vallee, L.M. Artner, J. Darnedde, C.P.R. Hackenberger, Alkyne phosphonites for sequential azide-azide couplings, *Angew. Chem.-Int. Ed.* 52 (36) (2013) 9504–9508.
- [40] A. Dag, H. Sahin, H. Durmaz, G. Hizal, U. Tunca, Block-Brush Copolymers via ROMP and sequential double click reaction strategy, *J. Polym. Sci. Part A-Polym. Chem.* 49 (4) (2011) 886–892.
- [41] F. Sonmez, B.Z. Kurt, I. Gazioglu, L. Basile, A. Dag, V. Cappello, T. Ginex, M. Kucukislamoglu, S. Guccione, Design, synthesis and docking study of novel coumarin ligands as potential selective acetylcholinesterase inhibitors, *J. Enzyme Inhib. Med. Chem.* 32 (1) (2017) 285–297.
- [42] A.R.G. Khalifah, The carbon dioxide hydration activity of carbonic anhydrase. I. Stop-flow kinetic studies on the native human isoenzymes B and C, *J. Biol. Chem.* 246 (1971) 2561–2573.
- [43] (a) A. Maresca, C. Temperini, H. Vu, N.B. Pham, S.A. Poulsen, A. Scozzafava, R.J. Quinn, C.T. Supuran, Non-Zinc mediated inhibition of carbonic anhydrases: coumarins are a new class of suicide inhibitors, *J. Am. Chem. Soc.* 2009, 131, 3057–3062; (b) A. Maresca, C.T. Supuran, Coumarins incorporating hydroxy- and chloro-moieties selectively inhibit the transmembrane, tumor-associated carbonic anhydrase isoforms IX and XII over the cytosolic ones I and II, *Bioorgan. Med. Chem. Lett.* 2010, 20, 4511–4514.
- [44] (a) C.T. Supuran, A. Nikolae, A. Popescu, Carbonic Anhydrase Inhibitors. Part 35. Synthesis of Schiff bases derived from sulfanilamide and aromatic aldehydes: the first inhibitors with equally high affinity towards cytosolic and membrane-bound isozymes, *Eur. J. Med. Chem.* 31 (1996) 431–438; (b) F. Carta, M. Aggarwal, A. Maresca, A. Scozzafava, R. McKenna, E. Masini, C.T. Supuran, Dithiocarbamates strongly inhibit carbonic anhydrases and show anti-glioma action in vivo, *J. Med. Chem.* 55 (2012) 1721–1730.
- [45] a) A. Maresca, A. Scozzafava, C.T. Supuran, 7,8-disubstituted but not 6,7-disubstituted coumarins selectively inhibit the transmembrane, tumor-associated carbonic anhydrase isoforms IX and XII over the cytosolic ones I and II in the low nanomolar/subnanomolar range, *Bioorg. Med. Chem. Lett.* 20 (2010) 7255–7258; b) C. Temperini, A. Innocenti, A. Scozzafava, S. Parkkila, C.T. Supuran, The coumarin-binding site in carbonic anhydrase accommodates structurally diverse

- inhibitors: the antiepileptic lacosamide as an example and lead molecule for novel classes of carbonic anhydrase inhibitors, *J. Med. Chem.* 53 (2010) 850–854.
- [46] C. Temperini, A. Innocenti, A. Scozzafava, S. Parkkila, C.T. Supuran, The coumarin-binding site in carbonic anhydrase accommodates structurally diverse inhibitors: the antiepileptic lacosamide as an example and lead molecule for novel classes of carbonic anhydrase inhibitors, *J. Med. Chem.* 53 (2) (2009) 850–854.
- [47] B.P. Mahon, A. Bhatt, L. Socorro, J.M. Driscoll, C. Okoh, C.L. Lomelino, M.Y. Mboge, J.J. Kurian, C. Tu, M. Agbandje-McKenna, S.C. Frost, R. McKenna, The structure of carbonic anhydrase IX is adapted for low-pH catalysis, *Biochemistry* 55 (33) (2016) 4642–4653.
- [48] A. Zubrienė, A. Smirnov, V. Dudutienė, D.D. Timm, J. Matulienė, V. Michailovienė, A. Zakšauskas, E. Manakova, S. Gražulis, D. Matulis, Intrinsic thermodynamics and structures of 2, 4-and 3, 4-substituted fluorinated benzenesulfonamides binding to carbonic anhydrases, *ChemMedChem* 12 (2) (2017) 161–176.
- [49] G.M. Sastry, M. Adzhigirey, T. Day, R. Annabhimoju, W. Sherman, Protein and ligand preparation: parameters, protocols, and influence on virtual screening enrichments, *J. Comput. Aided Mol. Des.* 27 (3) (2013) 221–234.
- [50] D.C. Bas, D.M. Rogers, J.H. Jensen, Very fast prediction and rationalization of pKa values for protein–ligand complexes, *Proteins Struct. Funct. Bioinf.* 73 (3) (2008) 765–783.
- [51] J.C. Shelley, A. Cholleti, L.L. Frye, J.R. Greenwood, M.R. Timlin, M. Uchimaya, Epik: a software program for pKa prediction and protonation state generation for drug-like molecules, *J. Comput. Aided Mol. Des.* 21 (12) (2007) 681–691.
- [52] E. Harder, W. Damm, J. Maple, C. Wu, M. Reboul, J.Y. Xiang, L. Wang, D. Lupyan, M.K. Dahlgren, J.L. Knight, J.W. Kaus, D.S. Cerutti, G. Krilov, W.L. Jorgensen, R. Abel, R.A. Friesner, OPLS3: a force field providing broad coverage of drug-like small molecules and proteins, *J. Chem. Theory Comput.* 12 (1) (2016) 281–296.
- [53] Schrödinger, LLC, New York, NY, 2017.
- [54] Desmond Molecular Dynamics System, D. E. S. R., New York, NY, 2017. Maestro-Desmond Interoperability Tools, Schrödinger, New York, NY, 2017.
- [55] Schrödinger, LigPrep, S., LLC, New York, NY, 2017.
- [56] G. Jones, P. Willett, R.C. Glen, A.R. Leach, R. Taylor, Development and validation of a genetic algorithm for flexible docking, *J. Mol. Biol.* 267 (3) (1997) 727–748.
- [57] M.L. Verdonk, G. Chessari, J.C. Cole, M.J. Hartshorn, C.W. Murray, J.W.M. Nissink, R.D. Taylor, R. Taylor, Modeling water molecules in protein–ligand docking using GOLD, *J. Med. Chem.* 48 (20) (2005) 6504–6515.
- [58] O. Korb, T. Stützel, T.E. Exner, Empirical scoring functions for advanced protein–ligand docking with PLANTS, *J. Chem. Inf. Model.* 49 (1) (2009) 84–96.